https://ntrs.nasa.gov/search.jsp?R=19680013419 2020-03-12T08:57:10+00:00Z

VL-2438-14-O

FINAL REPORT

DEVELOPMENT OF A 50 kW FLUID TRANSPIRATION ARC SOLAR SIMULATOR

by

D. R. Simon

November 1967

Prepared for

National Aeronautics Space Administration
Manned Spacecraft Center
Space Environmental Simulation Branch
Houston, Texas

Under contract

NAS 9-5726

GPO PRICE $ _____

CFSTI PRICE(S) $ _____

Hard copy (HC) 3.00

Microfiche (MF) .65

ff 653 July 65

MAY 1968
RECEIVED
NASA STI FACILITY
INPUT BRANCH

Vitro LABORATORIES
DIVISION OF VITRO CORPORATION OF AMERICA
200 Pleasant Valley Way, West Orange, N. J.

FACILITY FORM 602

N68-22888 (ACCESSION NUMBER) (THRU) 1

46 (PAGES) (CODE)

NASA-CR-92067 (NASA CR OR TMX OR AD NUMBER) 1 (CATEGORY)

NASA CR 92067

VL-2438-14-O

FINAL REPORT

DEVELOPMENT OF A 50 kW FLUID TRANSPIRATION ARC SOLAR SIMULATOR

by

D. R. Simon

November 1967

Prepared for

National Aeronautics Space Administration
Manned Spacecraft Center
Space Environmental Simulation Branch
Houston, Texas

Under contract

NAS 9-5726

Vitro LABORATORIES DIVISION OF VITRO CORPORATION OF AMERICA

WEST ORANGE LABORATORY • 200 Pleasant Valley Way, West Orange, N. J.

TABLE OF CONTENTS

		Page
1.	ABSTRACT	1
2.	INTRODUCTION	2
3.	RADIATION SOURCE	3
	3.1 FTA Arc Head Development	3
	3.2 FTA Arc Performance Data	12
4.	SUPPORT MODULE	15
	4.1 Gas Recirculation	15
	4.2 Water Cooling System	15
	4.3 Getter Design	19
	4.4 Control Circuitry	20
5.	QUARTZ DOME DEVELOPEMENT	25
	5.1 Calculation of Hydrostatic and Thermal Stress in a Dome-Shaped Envelope	25
	5.2 Quartz Enclosure Performance	31
	5.3 Fused Seal Studies	35
6.	SUMMARY AND CONCLUSIONS	39
7.	REFERENCES	41

LIST OF ILLUSTRATIONS

Figure	Title	Page
1	Anode and Cathode Arrangement With Enclosure Seal (38 kW Test Configuration)	4
2	Cathode Configuration	4
3	Experimental Fluid Transpiration Arc Head	6
4	FTA at 31 kW and 80 psi	6
5	Highly Eroded Anode as a Result of Minute Water Leaks	7
6	Assembly Sketch of FTA Head Indicating the the Location of Solder Failure	7
7	Solder Failure Due to Melting at 43 kW in Anode Joint	9
8	FTA Head Assembly	10
9	Insulation	11
10	Anode Arrangement	11
11	Cathode	11
12	Spectral Intensity Distribution at 38.5 kW	13
13	Spectral Intensity Distribution at 48.2 kW	13
14	Brightness Profile For FTA Source	14
15	Lapp Pulse Feeder Model CPS-2	16
16	Gas Purifier System and Recirculation Pump	17
17	Argon Recirculation System Calibration	17
18	Rotometer Calibration Indicating Argon Mass Flow as a Function of Pressure and Rotometer Reading	18
19	Water Coolant System	18
20	Two Stage Zirconium Getter	21

LIST OF ILLUSTRATIONS (Continued)

Figure	Title	Page
21	Support Module Layout (Right Side View)	22
22	Control Module Circuitry	23
23	Remote Control Circuit	24
24	Quartz Envelope Dimension	26
25	Quartz Failure After One Minute at 18 kW	32
26	Quartz Failure Due to Mechanical Stress Points	32
27	Quartz Dome After Silicone Gasket Failure	34
28	End View Showing the Degraded Seal and Quartz Dome	34
29	Inconel-X V-ring Seal Design	36
30	Redesigned 50 kW Arc Head and Seal Configuration	37
31	Assembled Unit Prior to Test Run	38
32	Proposed System for NASA-MSC Solar Simulator	40

1. ABSTRACT

An engineering model of a Fluid Transpiration Arc has been designed, developed, and built. A complete supporting system including controls and interlocks, water cooling apparatus, a high voltage striker, a gas recirculator, and a gas purifier was designed and built. A quartz dome to enclose the arc head was developed and tested. After several tests showed that epoxy bonding and silicone rubber gaskets were not satisfactory dome seals at the temperatures encountered, a successful dome seal design using a metallic V-ring was demonstrated.

One test of the redesigned arc head, which was scaled up from a 25 kW unit with a 50 hour lifetime, demonstrated a lifetime of 107 hours in continuous operation at an input level of 40 to 45 kW. No adjustment or maintenance was required during that run and the arc stability was excellent. During the 107 hour run which was made with the arc inside a water cooled enclosure, various measurements of radiant output were taken. These measurements indicate a source size of approximately 1 cm diameter at 42 kW with an output of 1.34 kW/steradian at 100 psi in argon. Several subsequent tests were then made with the arc operating inside a close-fitting quartz dome; the useful life of the arc was shortened during these tests due to a greatly increased rate of electrode erosion. Deposition of electrode material on the quartz dome reduced the light output severely in a few hours of operation at 40 kW input.

A design is proposed for enclosing both the collecting optics and the arc head assembly in a pressurized tank thus avoiding the need for a close-fitting dome on the arc head itself.

2. INTRODUCTION

Considerable effort in recent years has gone into the development of efficient, high power arc sources of radiant energy. All of the units have serious heat dissipation problems at the anode which, in general, limits radiant output and lifetime.

The Fluid Transpiration Arc (FTA) configuration has one of the lowest anode power densities of all the devices currently in the development stage. The arc also has the smallest radiant source size for the equivalent power of any of the current sources. For these reasons, a 50 kW solar simulation module completely interchangeable with the current module was undertaken. Improvements in uniformity, power output and reliability were reasonable expectations. One of the goals of the program was a 200 hour longevity run of the FTA within a quartz dome. This goal was not reached due to convection current problems introduced by the small confines of the quartz enclosure. An arc lifetime of 107 hours in continuous operation at an input level of 40 to 45 kW was demonstrated with an FTA operating within a water-cooled metallic enclosure. The development of a system which points directly towards a successful module design was completed, however, and the arc source and support system design has been successfully completed.

This report summarizes the development work performed on the 50 kW Fluid Transpiration Arc system performed under contract NAS9-5726. We wish to thank Mr. P. Vincent#ES6 of NASA-MSC for his patience and useful suggestions during the more difficult development phases of the program.

3. RADIATION SOURCE

3.1 FTA Arc Head Development

The successful design of a 50 kW FTA depended upon the proper extrapolation of previous lower power designs. Original investigations at Vitro Laboratories studying fluid transpiration through the anodic boundary were carried out between 1958 and 1961 at power levels below 10 kW.[1] Following these studies a concentrated effort supported by AEDC[2] carried the development of the concept to an engineering level which culminated with a 50 hour run at 25 kW. Although several major problem areas required solution before the arc could successfully be brought to the 50 kW - 200 hour lifetime in quartz operating level, these problems seemed solvable, and the program to achieve this end was initiated.

The first step taken towards these goals was the design of a unit which operated at 38 kW and provided scoping data for the following design of a closed loop prototype which has run to 80 kW for short periods, and between 40 kW and 45 kW for 107 hours.

The initial arc head as shown in Figures 1 and 2 represents the first scale-up model, having a 1/2-inch diameter, 2% thoriated tungsten cathode, and mean anode diameter of 1.4-inches. This unit was tested without a shroud, and run up to 38 kW (38 volts and 1000 amperes) to check the preliminary water cooling requirement of 3 gal./min. anode flow. Based on the data taken during these first tests a 50 kW arc head was designed (Figure 3) using a water and gas-cooled copper anode, a boron nitride insulator, a thoriated tungsten cathode, and a water-cooled copper shroud. A small steel enclosure was constructed with three observation ports and internal water-cooling provisions for use as a testbed. The first significant problem encountered was related to system cleanliness and manifested itself as CuO and CuO_2 dust. The cleanliness problem was somewhat alleviated by using the following technique to clean the head before assembling the system:

1. Degrease in acetone.
2. Air dry.
3. 15 minute bath in a mixture of 7.5 pt. concentrated sulfuric acid and 92.5 pt. distilled water at 175 °F.
4. Wash in distilled water twice.
5. 10 second bath in mixture of 25 pt. concentrated sulfuric acid, 15 pt. concentrated nitric acid, 60 pt. distilled water, at room temperature.

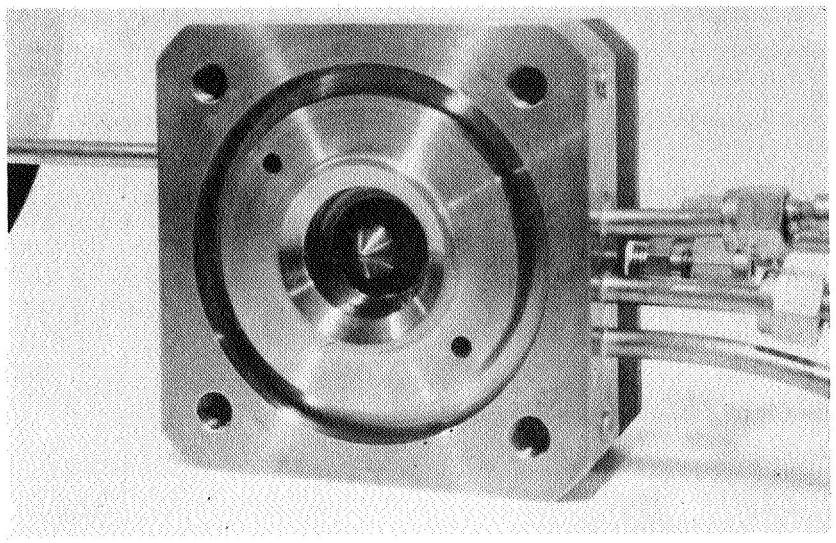

FIGURE 1

ANODE AND CATHODE ARRANGEMENT WITH ENCLOSURE SEAL (38 kW TEST CONFIGURATION)

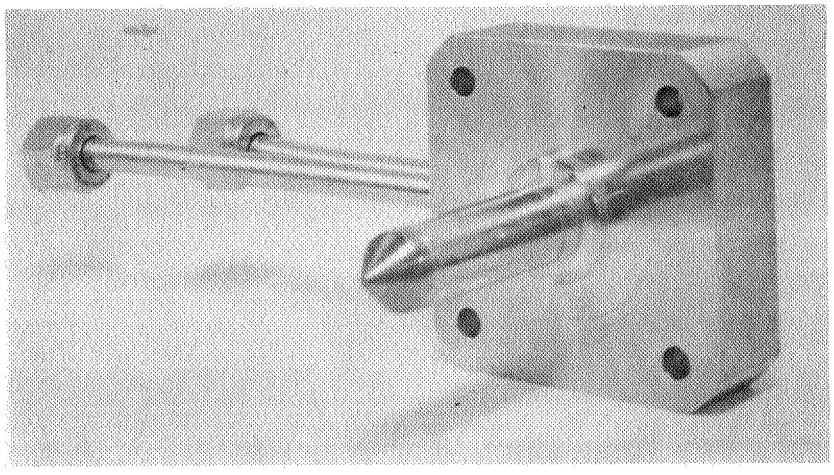

FIGURE 2

CATHODE CONFIGURATION

6. Wash in distilled water twice.
7. 10 to 20 second dip in 40 pt. concentrated sulfuric acid, 20 pt. concentrated nitric acid, 10 pt. distilled water, 0.3 pt. concentrated hydrochloric acid.
8. Wash in hot distilled water twice.
9. Rinse in denatured alcohol
10. Air dry.
11. Vacuum bake.

After vacuum bakeout of the chamber the system performed without the generation of the copper oxides unless there existed an accompanying failure in the insulator or water circulation system.

The 50 kW head discussed above was designed with high temperature "O" ring seals to provide for easy maintenance and inexpensive replacement of components. After a 5 hour run, starting at 31 kW and then gradually increasing to 40 kW, a failure of one of the "O" ring seals was noted, and the subsequent degradation of the arc head was attributed to this cause. The arc head design was modified to eliminate this problem by using silver-soldered joints in fabrication. A series of six runs were made on this unit to debug the new design for an extended operation test. A photograph of the unit in operation is shown in Figure 4.

The first two tests in this series were terminated because of excessive pulsation and oxygen content resulting in rapid cathode erosion. These problems were reduced in magnitude by installing additional damping in the gas recirculation system and vacuum baking the arc enclosure for a 24-hour period. The cathode showed no degradation during the following tests at a 1200 ampere level. During the second of these tests the anode built up a heavy layer of copper oxide which was also eliminated in subsequent tests. The third and fourth tests were terminated due to minute water leaks in the soldered joints which were not detected during the visual 350 psi water pressure checks. The degradation of the anode due to these leaks can be seen in Figure 5. A more sensitive method of leak detection was perfected and the above mentioned failure modes eliminated by disassembly, thorough cleaning, and very careful resoldering of the defective seal. The fifth and sixth runs were carried out on the same head. The fifth run consisted of a low power checkout at levels up to 30 kW for 2.5 hours. This run was terminated and all the components checked and cleaned for the sixth test. This experiment ran for 3 hours at 40-43 kW before a failure in an internal solder joint caused a shutdown. The joint which failed was located over a bridge in the anode water-cooling channel, Figure 6, and

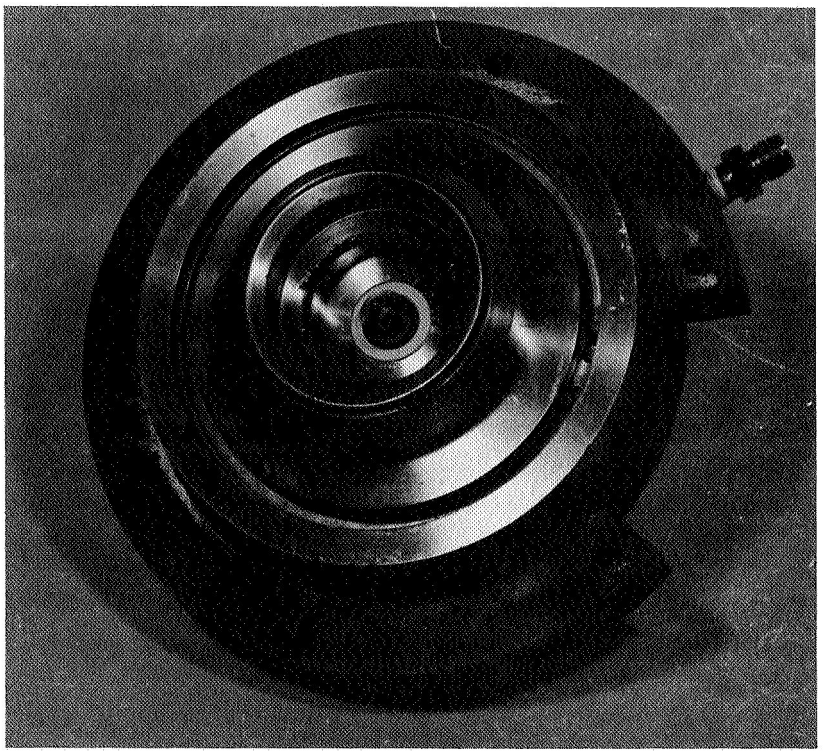

FIGURE 3

EXPERIMENTAL FLUID TRANSPIRATION ARC HEAD

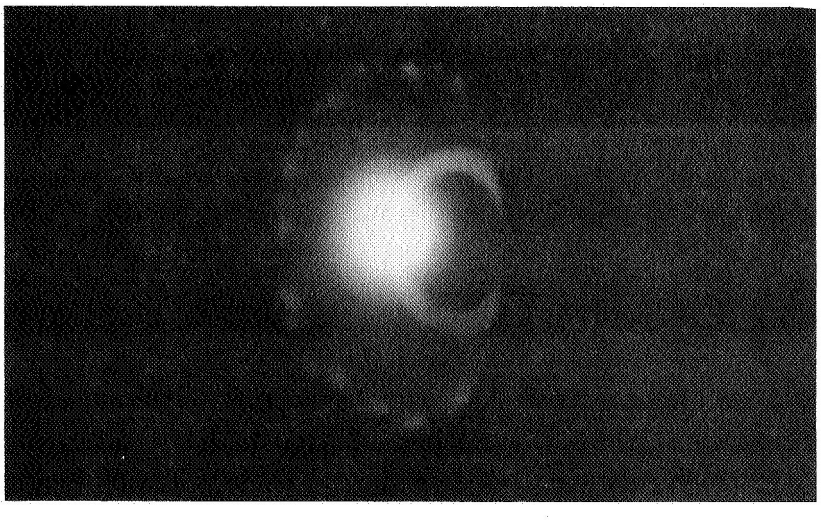

FIGURE 4

FTA AT 31 kW AND 80 PSI

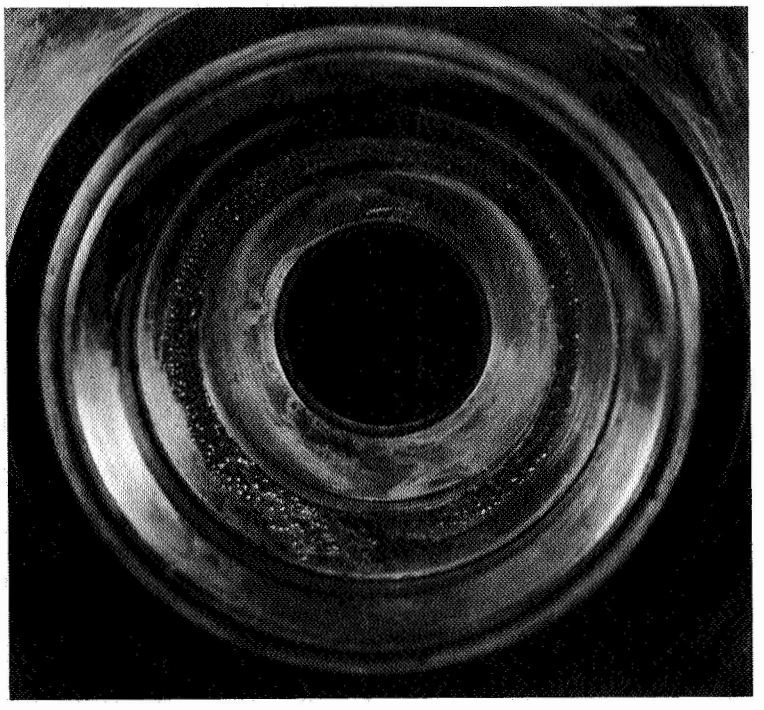

FIGURE 5

HIGHLY ERODED ANODE AS A RESULT OF MINUTE WATER LEAKS

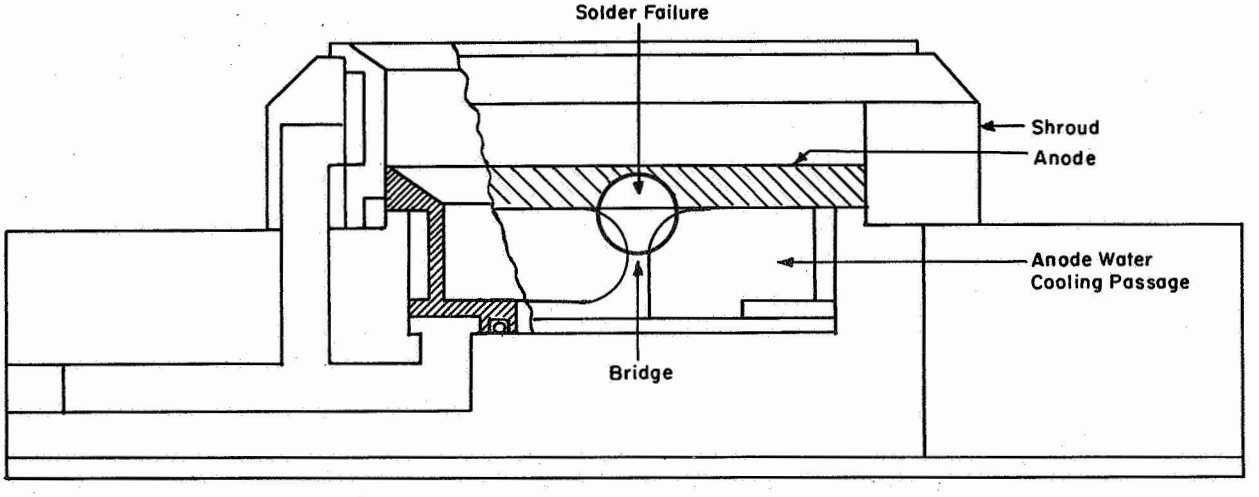

FIGURE 6

ASSEMBLY SKETCH OF FTA HEAD INDICATING THE LOCATION OF SOLDER FAILURE

showed evidence of melting (1100 °F), Figure 7. This problem was rectified by a modification of the bridge and a relocation of the channel. This modified design was assembled using the prescribed cleaning techniques prepared for a longevity run. After 671.8 minutes of operation at power levels up to 43 kW a water leak appeared in the external tubing. This was due to a split line and made it mandatory to immediately shut down. At this time the head was examined and a degradation of the boron nitride insulator was noted. The degradation had affected the cathode and we therefore changed this component for a new one. The recharged unit, however, only ran to a total of 731 minutes before continued insulator breakdown forced a shutdown in the test. The last test on this series of head designs was initiated on October 19, 1966, and differed in the previous run only in the fact that the boron nitride was baked out at 800 °C in a 10^{-6} torr vacuum. The experiment proceeded to 1530 minutes at a relatively constant power level. At this time the system was shut down to recharge the argon gas supply and then restarted. After restart the boron nitride degraded steadily and finally caused a shutdown at 1694 minutes. Based on these results an optimized head was designed and constructed incorporating the water cooling channel for the quartz dome and a redesigned boron nitride separator. This design is summarized in the drawing included as Figure 8.

The test on this unit proceeded to 1060 minutes between power levels of 40 and 50 kW and was terminated in order to examine the parts for degradation and not due to any system failures. The cathode showed a 0.0156 inch decrease in length, which was attributed to deformation of the tungsten tip under the 1300 ampere current load, and not to cathode erosion. The anode was somewhat pitted, although no signs of imminent failure were discernible. No degradation of the boron nitride was evident indicating that the design change had eliminated that weak link in the system. Preliminary tests were then performed in preparation for a 200 hour endurance test. The complete system was run between 53.0 and 55.0 kW for 101 minutes before a silicone rubber seal failure on the zirconium getter tank blew out causing termination.

An endurance test of the arc head alone was performed using welding-grade argon and a power input - between 40 and 45 kW. The arc head operated satisfactorily without interruption and completely without maintenance for 107 hours at which time a very minute water leak developed in the anode terminating the test. The failure occurred due to erosion and pitting of the copper anode by the arc. The tungsten cathode suffered some erosion but did not appear to be near failure. The boron nitride insulator, originally a troublesome component of the arc head, was discolored but was still in good operating condition. Figures 9, 10 and 11 are photographs of these components taken after the 107 hour run; the anode had been wiped clean to show

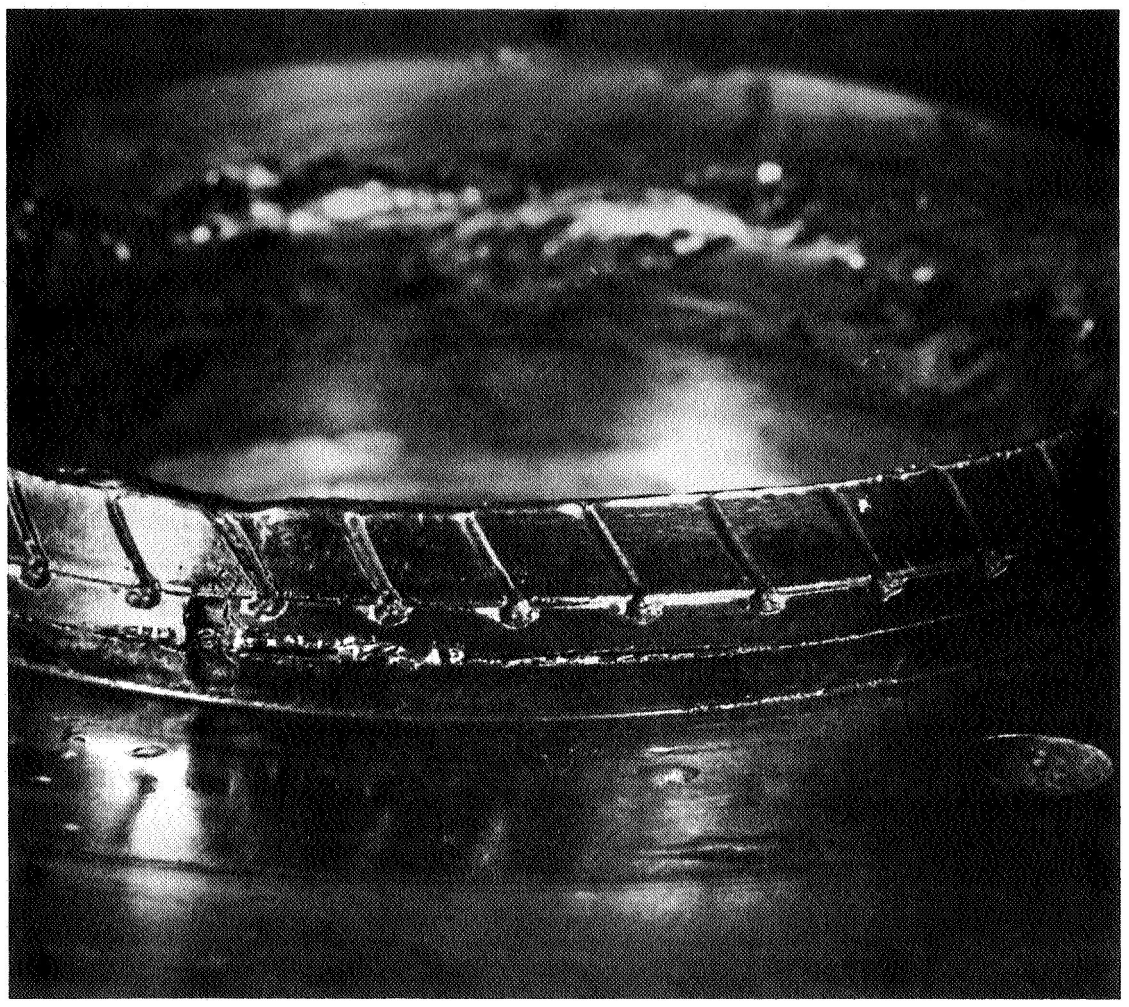

FIGURE 7

SOLDER FAILURE DUE TO MELTING

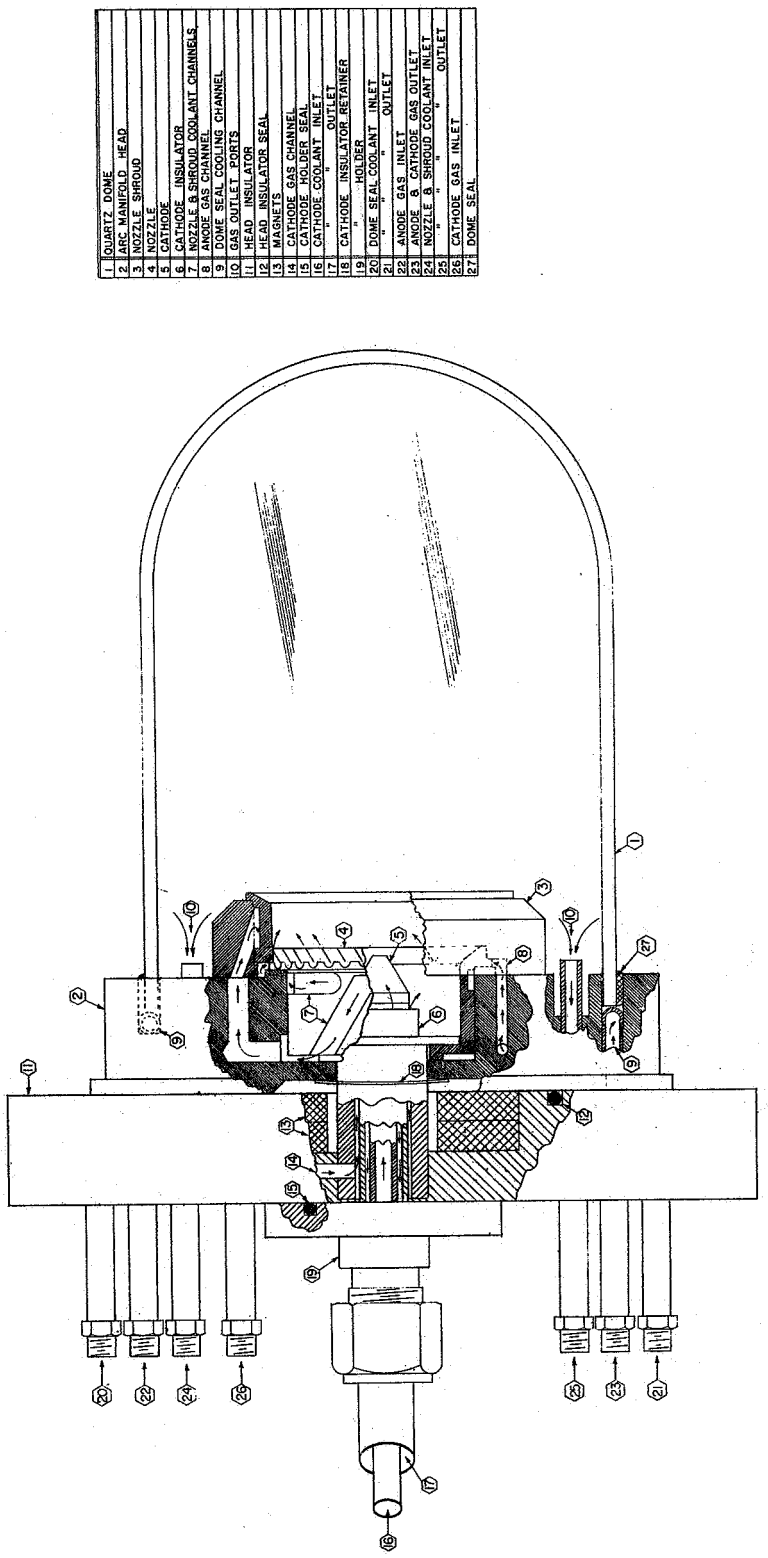

FIGURE 8

FTA HEAD ASSEMBLY

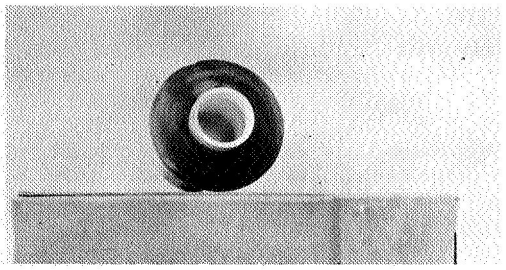

FIGURE 9

INSULATION

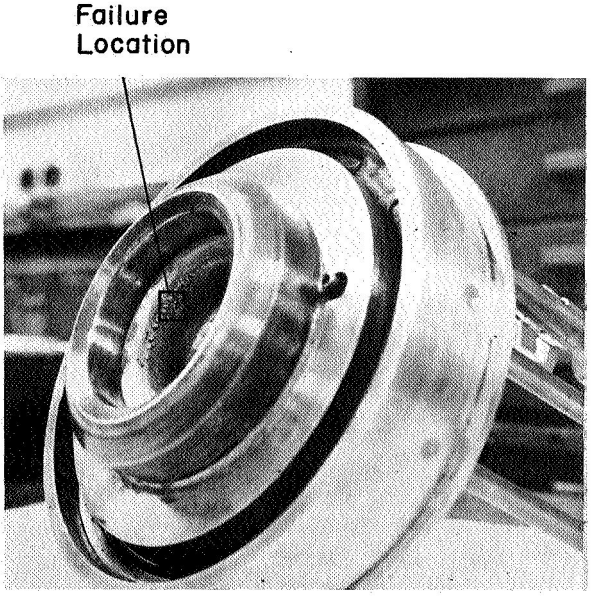

FIGURE 10

ANODE ARRANGEMENT

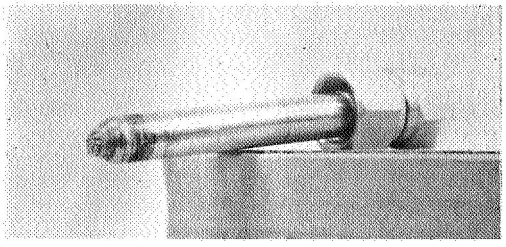

FIGURE 11

CATHODE

the erosion markings more clearly.

In order to perform a closed cycle test, the getter configuration was modified to a much more rugged and serviceable form that the initial model. Then end plates were water cooled to provide a heat sink for the hot zirconium elements. These same water cooled end plates were made power terminals and isolated by the quartz envelope. This unit was then incorporated into the system, and a closed loop 45 hour test was completed satisfactorily.

3.2 FTA Arc Performance Data

The spectral output of the FTA was measured with a Beckman DK-1 spectrophotometer using a NBS tungsten ribbon lamp #7041 as a standard of comparison. Relative spectral intensities as a function of wavelength are plotted in Figures 12 and 13 for a 38.5 kW, 60 psig argon FTA and 48.2 kW, 100 psig argon FTA respectively. An iso-brightness profile of the FTA was taken at 42.6 kW, 60 psig and is presented in Figure 14. The unit was tested for efficiency at various parameters using an Eppley thermopile, serial No. 6041, which develops a mean emf of 0.048 microvolts per microwatt per sq cm in its calibrated radiation range. The test was performed with an Infrasil window 1 mm thick on the chamber and a CaF_2 window 1 mm thick on the thermopile. Readings were taken at a distance of 100 cm from the cathode spot. The results of this series of tests are summarized in Table I.

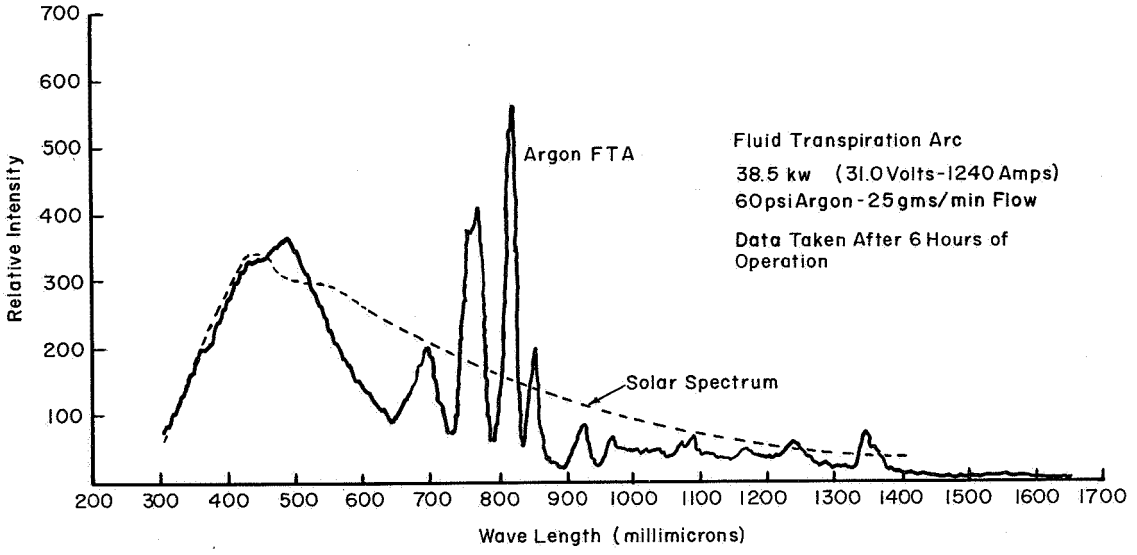

FIGURE 12

SPECTRAL INTENSITY DISTRIBUTION AT 38.5 kW

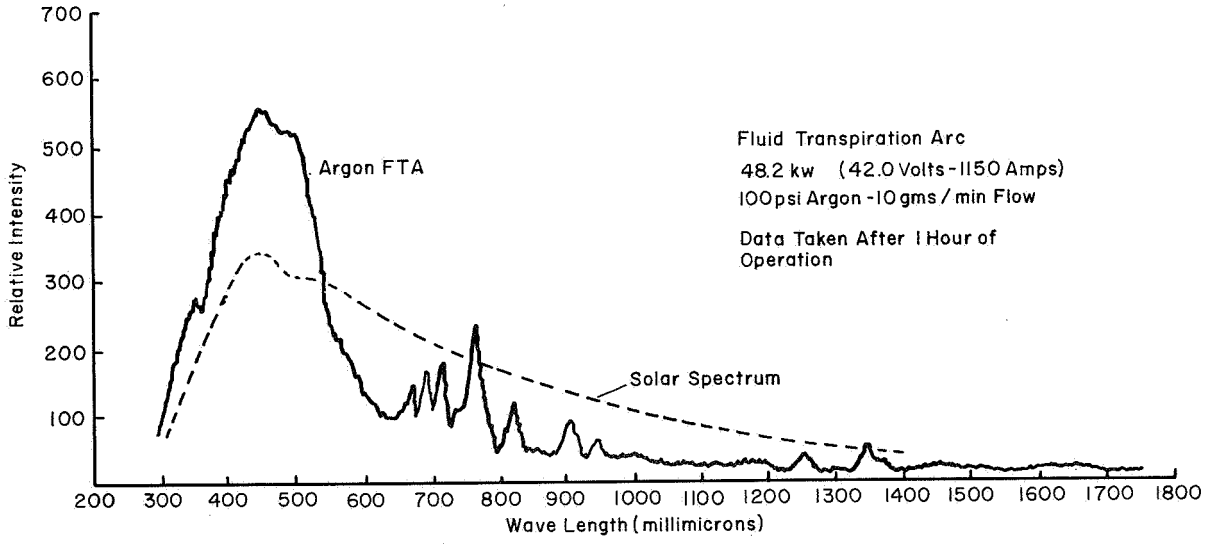

FIGURE 13

SPECTRAL INTENSITY DISTRIBUTION AT 48.2 kW

TABLE I

OPERATIONAL EFFICIENCY OF THE ARGON FTA

Arc Volts	Arc Current (amps)	Arc Power (kw)	Arc Pressure (psi)	Argon Flow (gms/min)	Radiant Power Out (2π steradians)	Efficiency (2π steradians)	Thermopile Output
35.0	800	28.0	60	8	4.7 kw	16.8%	3.6 mv
35.5	900	32.0	60	8	5.5 kw	16.7%	4.2 mv
35.0	1000	35.0	60	8	6.4 kw	18.3%	4.9 mv
35.0	1100	38.5	60	8	6.9 kw	17.9%	5.3 mv
35.5	1200	42.6	60	8	7.6 kw	17.8%	5.8 mv
42.0	600	25.2	100	10	5.4 kw	20.0%	4.1 mv
42.0	700	29.4	100	10	6.7 kw	22.8%	5.1 mv
42.0	750	31.5	100	10	7.3 kw	23.2%	5.6 mv
41.0	800	32.8	100	10	7.2 kw	22.0%	5.5 mv
41.0	900	37.0	100	10	7.8 kw	21.1%	6.0 mv
41.0	1000	41.0	100	10	8.2 kw	20.0%	6.2+ mv

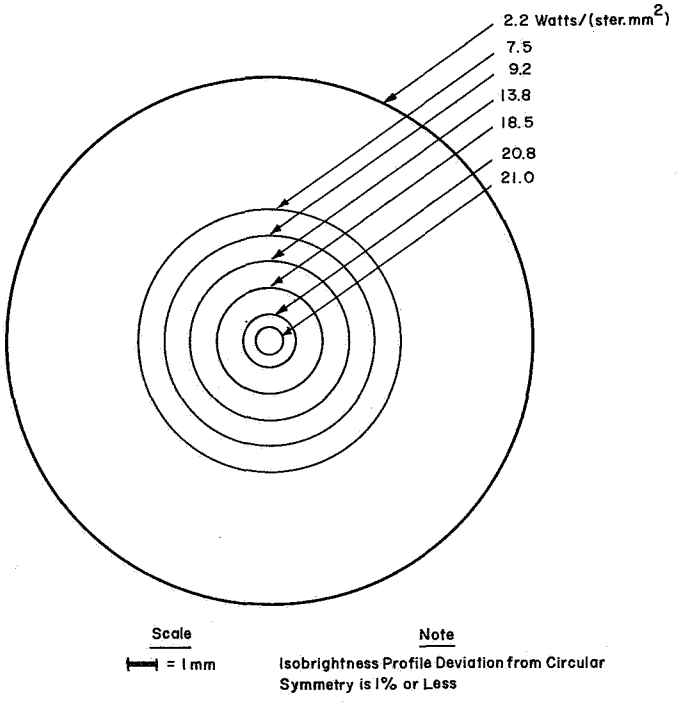

FIGURE 14

BRIGHTNESS PROFILE FOR FTA SOURCE

4. SUPPORT MODULE

The Fluid Transpiration Arc assembly requires various support operations which are contained in a module measuring 50" x 30" x 30". These operations are gas recirculation, gas cleaning, water cooling, safety controls and high voltage strike.

4.1 Gas Recirculation

The Gas recirculation is accomplished by a modified Lapp Pulsafeeder Pump, Model CPS-2, as shown in Figure 15. This pump belongs to a group classified as "positive displacement" pumps, wherein a diaphragm causes a displacement equal to the volume swept by the travel in the pumping head. Reciprocation of a piston in a cylinder hydraulically moves liquid against the diaphragm imparting perfect balance and allowing the diaphragm to follow the motion of the piston. Connected to the compression head is a hydraulic compensator pump, which provides excess hydraulic oil during each stroke. This assures the diaphragm contacting the front face of the stainless steel head on each stroke. The unit has been designed to operate at an inlet pressure of 150 psig and an outlet pressure of 150 psig with a capacity of 9 CFH argon gas. The swept volume of the head is 19.2 CFH giving a 50% pumping efficiency. The unit has a pulse rate of 300 ppm. Construction of the valves, seat material, gas head material and diaphragm material is SS 316. The valve gaskets are TFE, and the diaphragm gasket is a Buna N O-ring. The unit is driven by a 1-1/2 H.P. 220/440 volt, 60 cycle, 3-phase 1750 RPM totally enclosed motor.

The complete gas recirculation system as shown in Figure 16 consists of the pump, filters, arc head, and heat exchanger. It has been calibrated in terms of the system pressure and Pulsafeeder stroke to provide a flow rate without the use of a rotometer during an operational test. This calibration appears as Figure 17 along with the conversion curve, Figure 18, to indicate mass flow rate as a function of pressure and rotometer reading. Upon starting, the arc head is pumped down automatically to a low pressure (10 to 15 psia) to facilitate starting the arc. Upon striking the arc, the pressure is allowed to return to normal and gas circulation begins. The gettering action of the two-stage zirconium getter is initiated upon pumpdown to maintain a low gaseous impurity level.

4.2 Water Cooling System

The water coolant system (see Figure 19) is designed for a nominal 350 psi

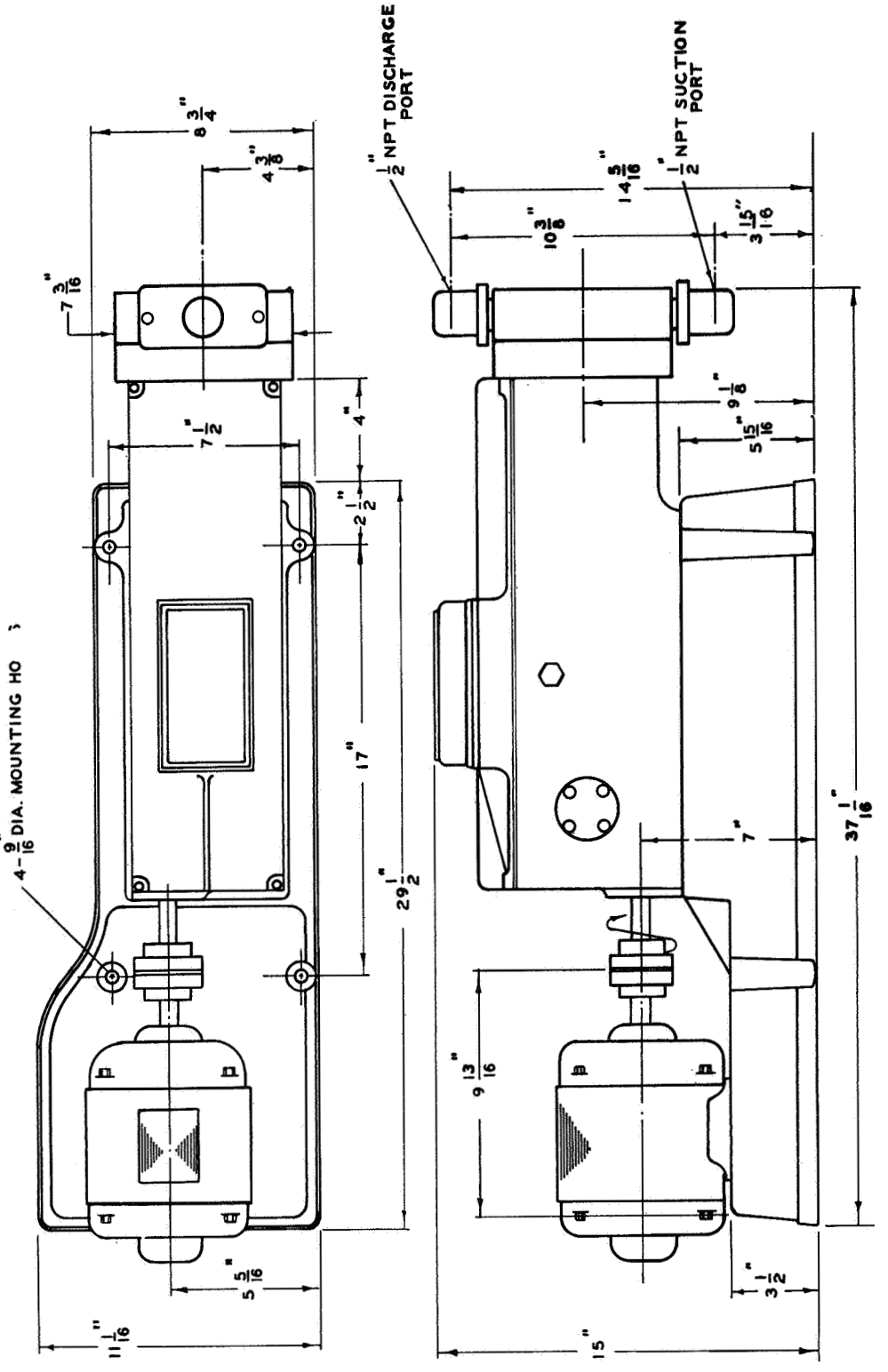

FIGURE 15

LAPP PULSE FEEDER MODEL CPS-2

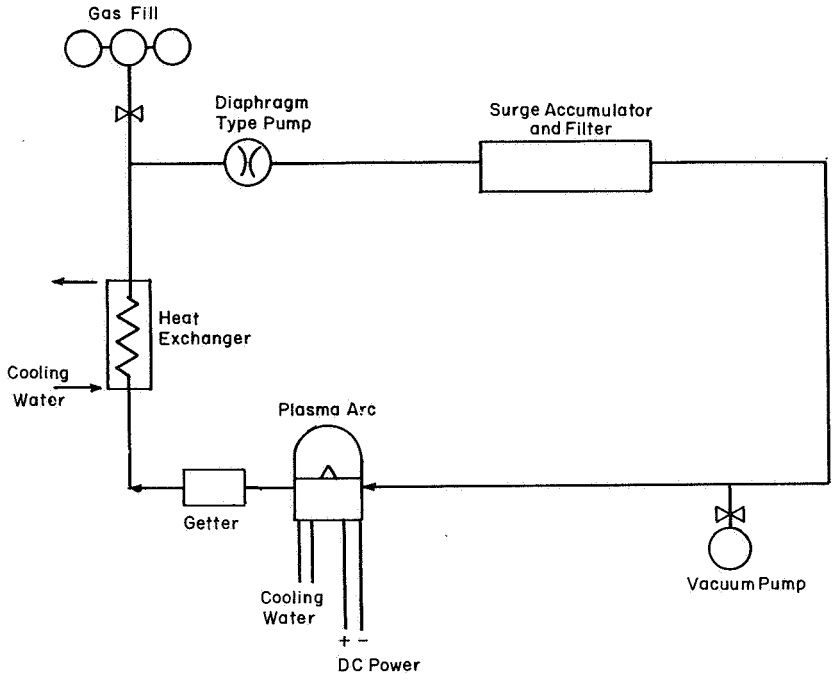

FIGURE 16

GAS PURIFIER SYSTEM AND RECIRCULATION PUMP

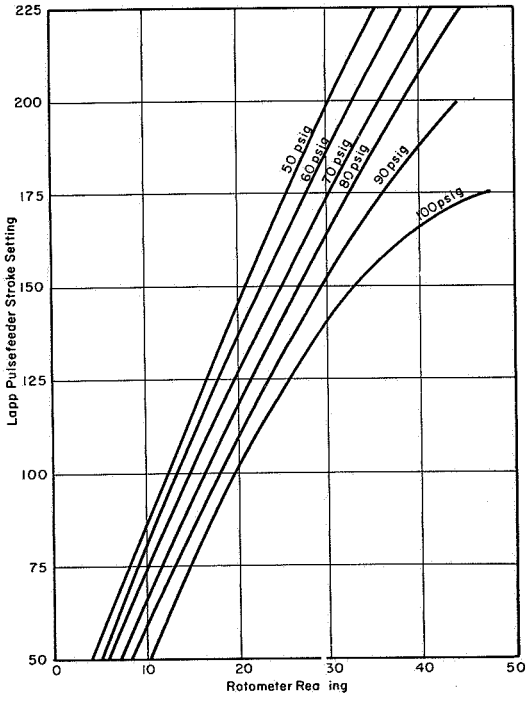

FIGURE 17

ARGON RECIRCULATION SYSTEM CALIBRATION

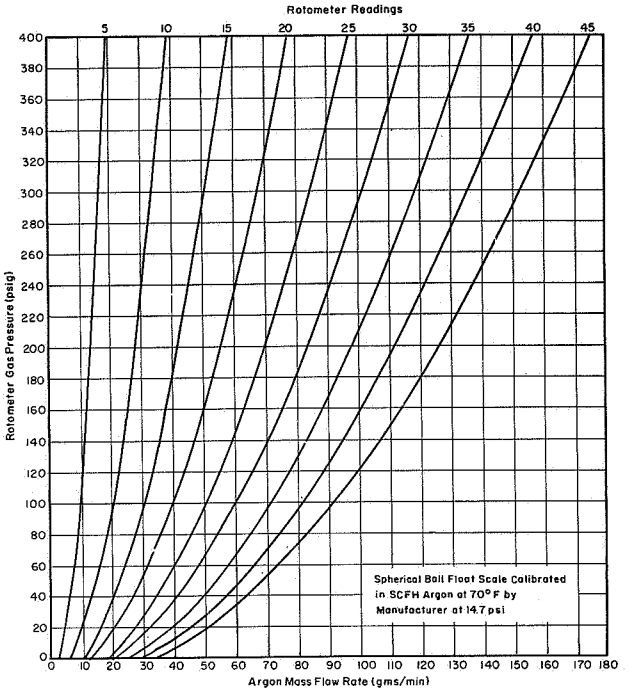

FIGURE 18

ROTOMETER CALIBRATION INDICATING ARGON MASS FLOW AS A FUNCTION OF PRESSURE AND ROTOMETER READING

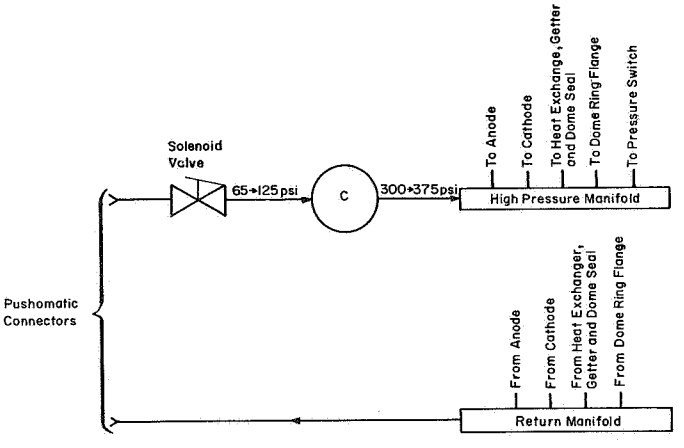

FIGURE 19

WATER COOLANT SYSTEM

pressure at a 70 psi inlet pressure. The high pressure water pump is a turbine type, close-coupled unit with a bronze impeller and sleeve. It is powered by a 5 H. P. 3-phase, 60 cycle motor with a rotational speed of 3500 RPM. The system is rated at a capacity of 3.5 gpm and is used to cool the anode and cathode, the return argon gas flow, the quartz dome seal and ring flange, and the zirconium getter.

4.3 Getter Design

The lifetime of the arc head will depend upon the concentration of impurities in the operating gas. In order to remove the gases which will be driven off from the metal surfaces during operation, a gettering arrangement was devised. Several materials were considered as to chemical activity and operating temperature and these are summarized for tantalum and zirconium.

Certain metals are capable of incorporating gases by solution into their bulk volume. An example of this is tantalum which, after degassing in a high vacuum for several hours at 1600 to 2000 °C, is capable of absorbing gases in amounts up to several hundred times its own volume. The optimum gettering temperature for tantalum is in the neighborhood of 1000 °C. At 1500 °C the gettering action begins to reverse. The main disadvantage of tantalum is the high temperature range required for proper degassing and subsequent gettering operation.

Zirconium has very desirable characteristics in that is forms very stable solid solutions with such gases as O, N. CO, and CO_2. Hydrogen is taken up very rapidly when the zirconium is heated to about 400 °C and it ceases to be sorbed at 500 °C. As the temperature is increased, the metal gives up hydrogen, but at 850 °C the hydrogen is then taken up due to a transition of zirconium. The solubility of oxygen, nitrogen, carbon compounds and hydrogen at high temperature is considerable. The temperature and volume relationship for the various gases (in micron liters/milligram) are as follows:

Oxygen	400 °C	1.99
Nitrogen	500 °C	1.00
Nitrogen	800 °C	1.46
Carbon monoxide	500 °C	0.43
Carbon monoxide	800 °C	3.65
Carbon dioxide	500 °C	0.57
Carbon dioxide	800 °C	3.04
Hydrogen	350 °C	13.33

Efficient oxygen sorption occurs throughout the range 200-800 °C, however, in the range 200 to 350 °C water vapor is also cleaned up about the same rate as oxygen.

The gettering arrangement originally used at the earlier stages in the system design is shown in Figure 20. Two double-coiled zirconium coils, wound on quartz mandrels were used, each designed to operate at a different temperature in order to take into account the variations in effective cleanup temperatures for the different impurities. One of the coils is operated at approximately 350 °C and the other at approximately 800 °C.

This configuration had problems with the current feedthroughs which overheated and cracked during system tests. The design was also difficult to assemble. A modified version used in the later tests had copper end plates which were water-cooled to remove the heat from the glowing zinconium wire. These same end plates were used as electrical terminals and isolated from each other by the quartz envelope and from the water-carrying tie rods by Ke 1-F insulations. The zirconium double-wound coils are wrapped aroung half-inch quartz tubes which have banana plugs at each end. These plug into the end plate assembly thereby reducing the service time for the getter to several hours.

4.4 Control Circuitry

The support module as shown in Figure 21 and contains a series of relays and safety switches which perform the start-stop functions and monitor the operation of the system. The control circuit for the module is described in Figure 22. The start switch (S1) activates relay (K1) which holds the power on as long as relay (K11) is unactivated. Relay (K2) and (K3) are activated by (K1) and start the high and low pressure water systems. Relay (K4) which is then activated by (K2) starts the gas recirculation system coupled with (K12) which senses the application of power to the gas pump motor. If the water pressure is approximately 350 psi then (K4) is also permitted to activate (K5). If the gas pressure is at the operational level, the K5 is allowed to activate (K6) which turns on the gettering system. The next step in the command chain is the activation of (K7) which turns on the power supplies to the FTA head. With the generators turned on, the next relay (K8), (which is a time delay unit and activated simultaneously with K7) kicks the striker on and a 20 kV, 3MHz signal breaks down the arc gap. (K9) which is activated by (K8) cuts out the striker after a predetermined period. If the lamp strikes, then (K12) is activated by a photodiode, and (K11) remains in its normally closed position. If the lamp is not struck, then (K13) does not activate K10 and the power is turned off preparatory to another start cycle. To provide remote control operation (see Figure 23) a remote control outlet is included to be wired to a main control panel for remote operation.

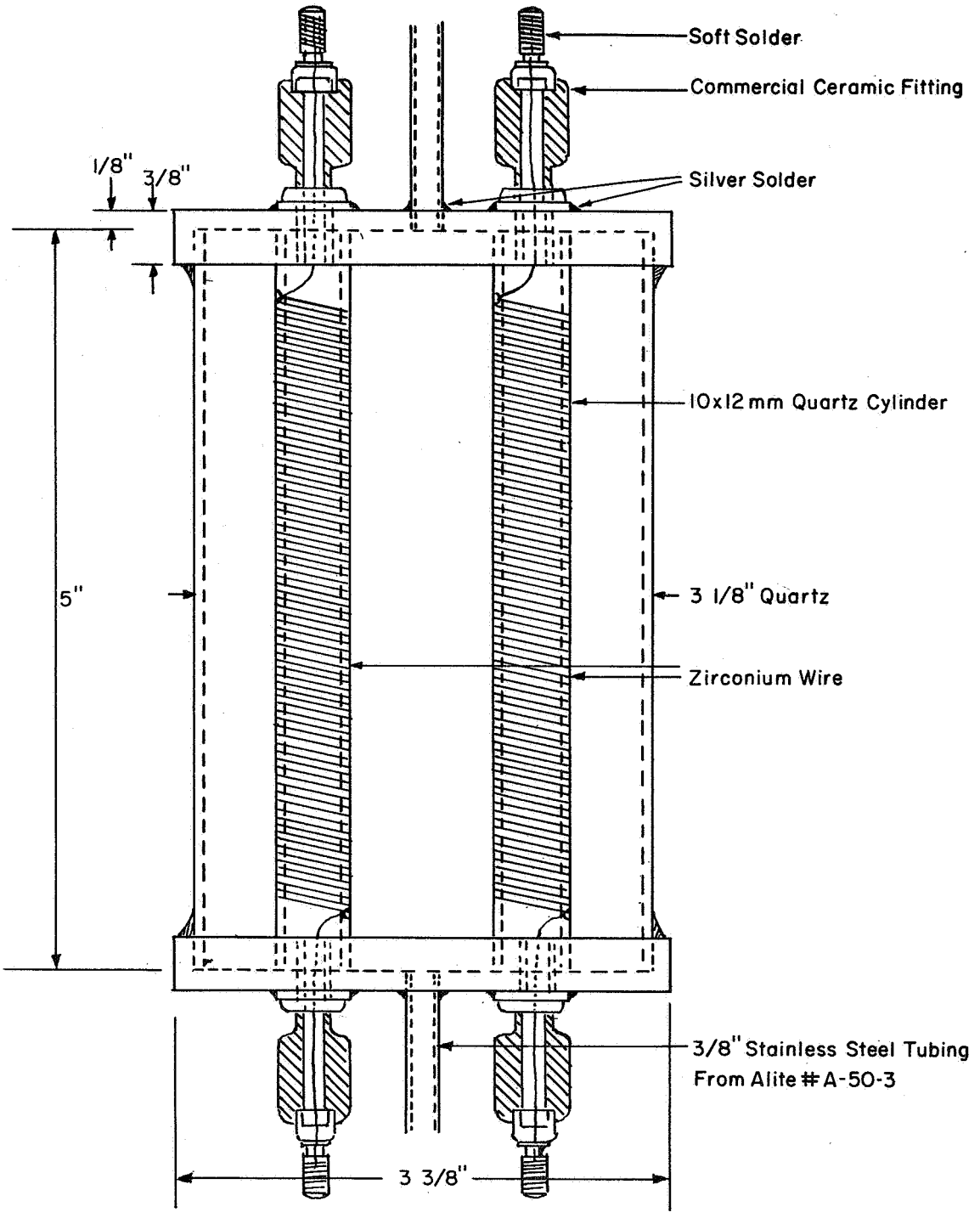

FIGURE 20

TWO STAGE ZIRCONIUM GETTER

K1, K2, K4, K6, K7

Potter & Brumfield
KRP 11A 115 V 50-60 C

K5, K9

Esna Agastat
Model No. 2112-A4SC

K8

Potter & Brumfield
CHB 38-70003

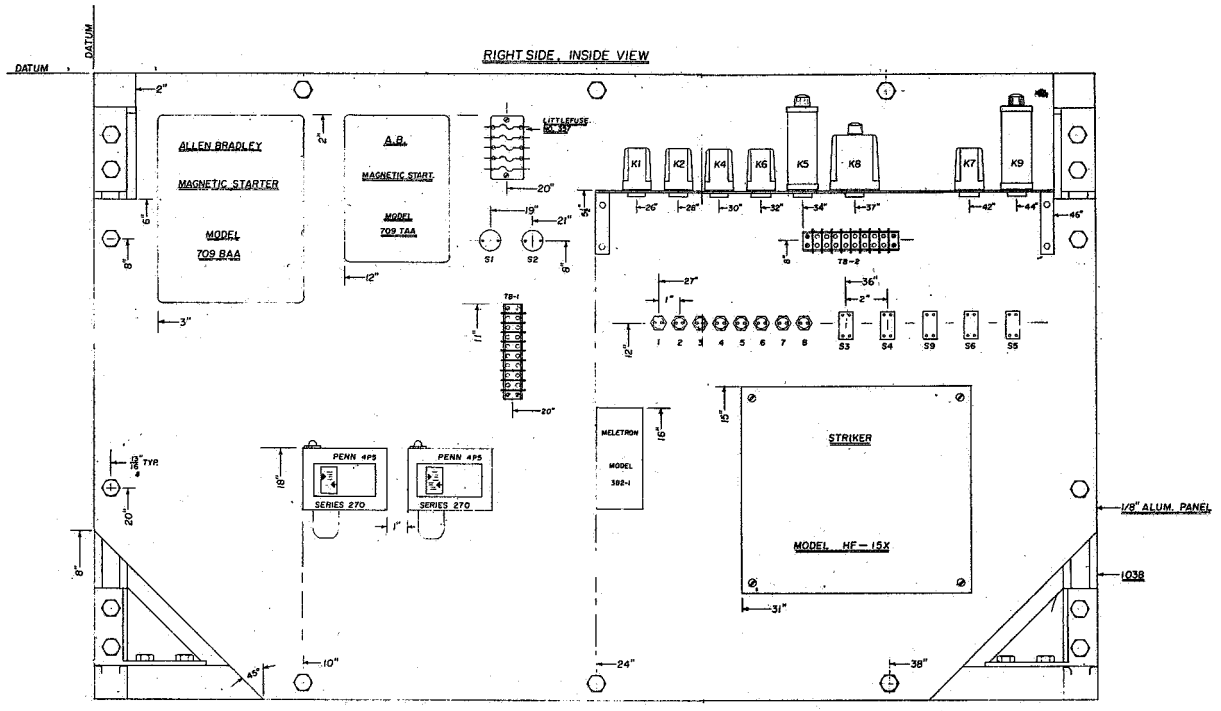

FIGURE 21

SUPPORT MODULE LAYOUT (RIGHT SIDE VIEW)

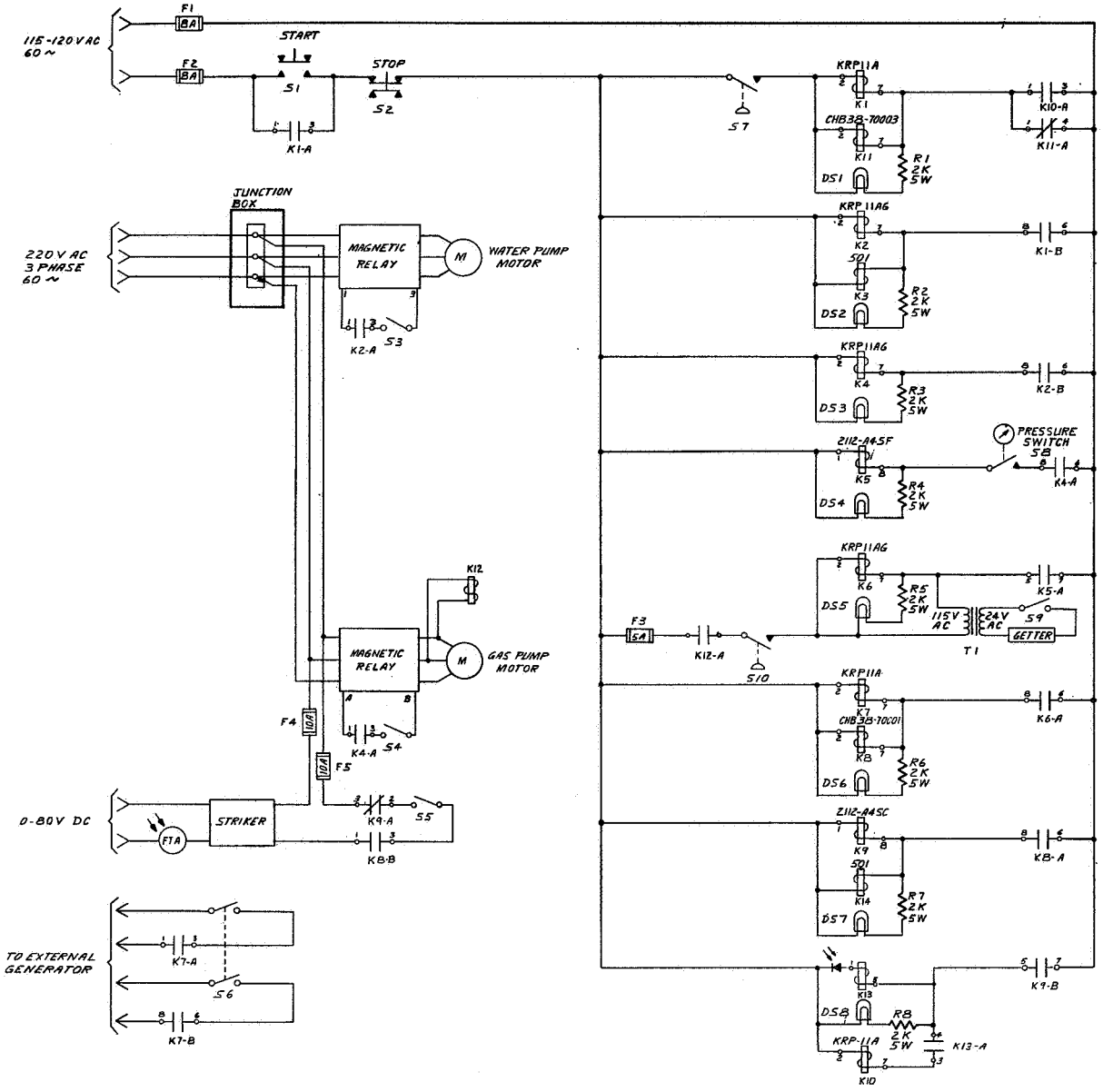

FIGURE 22

CONTROL MODULE CIRCUITRY

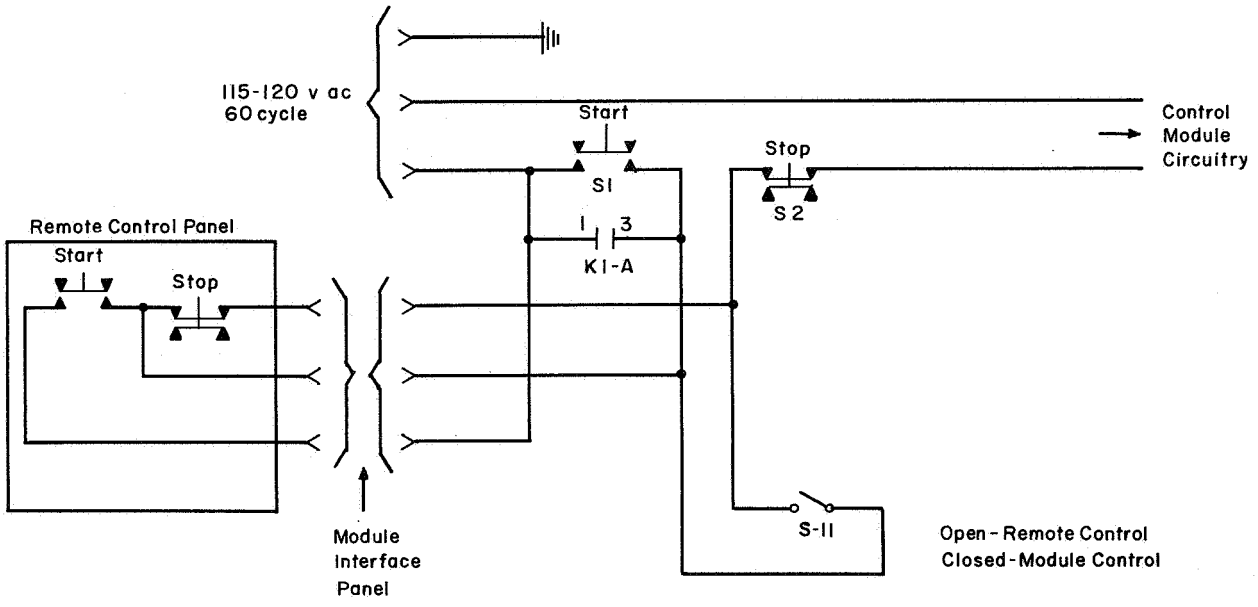

FIGURE 23

REMOTE CONTROL CIRCUIT

5. QUARTZ DOME DEVELOPMENT

In order to make use of the radiant output of the arc source, an enclosure compatible with the optical system at NASA Houston had to be developed. Initially it was felt that a quartz enclosure somewhat larger than the envelopes used in short arc lamps would be the most reasonable approach. Design and development of a quartz dome was then initiated.

5.1 Calculation of Hydrostatic and Thermal Stress in a Dome-Shaped Envelope

The computation of the hydrostatic and thermal stresses in the Fluid Transpiration Arc envelope can be performed by considering the envelope to be comprised of a perfect hemisphere joined to a cylinder with a uniform wall thickness. The configuration and dimensions for the 50 kW envelope are given in Figure 24.

Only a certain part of the total input power (W') consumed in the lamp is converted into radiation which is transferred out of the envelope without loss. Part is absorbed as radiation by the quartz and part by convection. The absorbed power heats the envelope to an operating temperature of 600-900C and creates a temperature gradient dT/dr which causes a thermal stress. This temperature gradient depends upon the total thermal power (W") that is conducted through the quartz wall per unit surface area as follows:

$$W'' = \gamma \frac{W'}{s} = \gamma W''' = - \lambda \frac{dT(r)}{dr}$$

where s is the area of irradiated surface, W''' is the average quartz surface loading, λ the termal conductivity of quartz, T(r) the temperature distribution within the quartz, and r the position as measured from the inner wall surface. For the purpose of calculating thermal stresses in this section the constant value $\gamma = 0.10$ is used. The following designations and numerical constants for clear fused quartz are used.

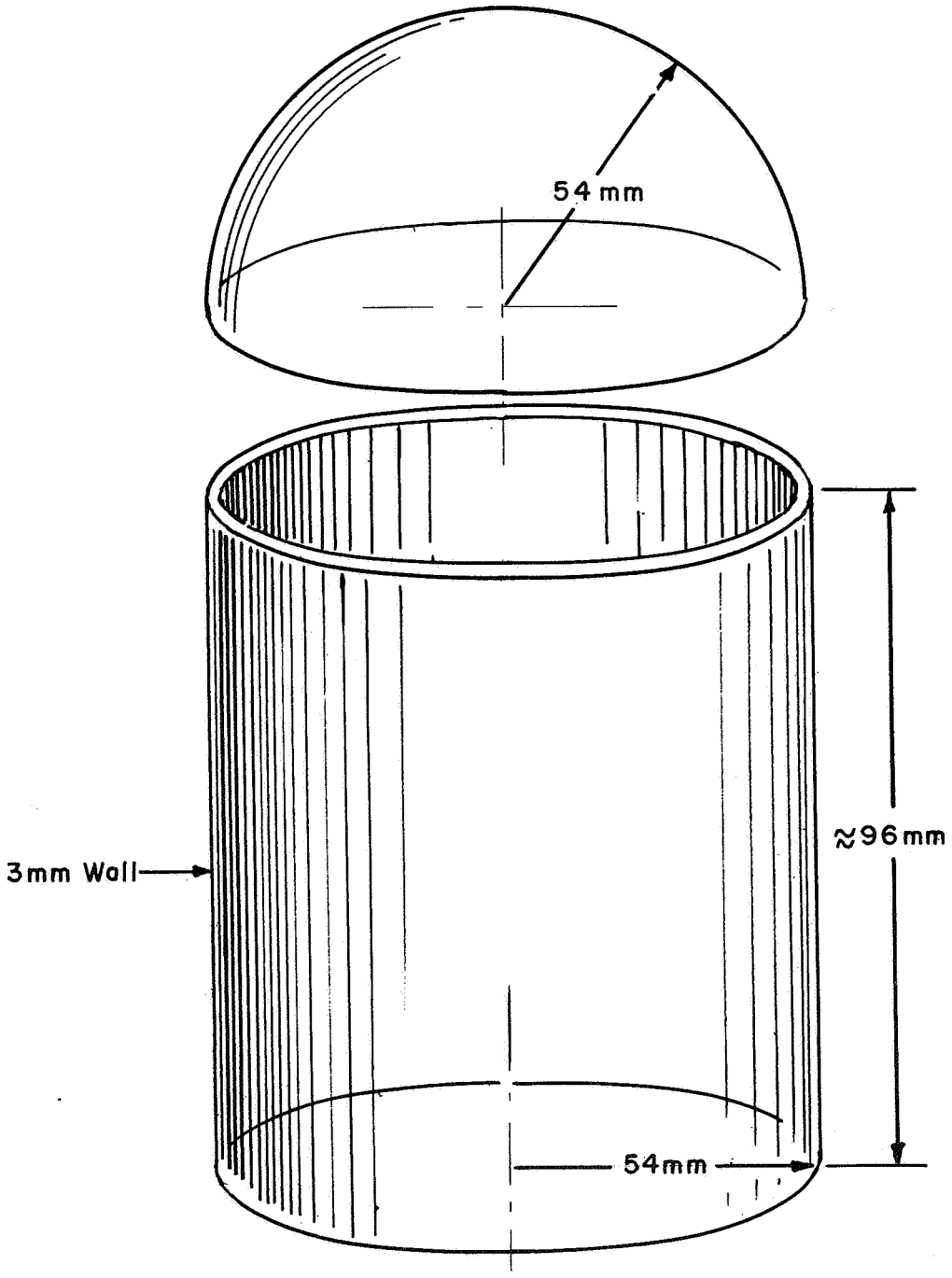

FIGURE 24

QUARTZ ENVELOPE DIMENSION

Coefficient of linear thermal expansion	$\alpha = 5.9 \times 10^{-7}\ ^{o}C^{-1}$
Heat conductivity (average between 0 and 600°C)	$\lambda = 0.17$ watts/deg cm
Modulus of elasticity	$E = 7 \times 10^{5}$ kg/cm^2 = 10^7 psi
Poisson's ratio	$\mu = 14 \times 10^{3}$ psi at 800 °C
Internal FTA operating pressure	P
Inner radius	r_i
Outer radius	r_o

The tensile stress within the cylindrical section can be described by two stress components

tangential component

$$\sigma^{c}_{P_e} = P\, r_i^{2} (r_o^{2} - r_i^{2})^{-1} (1 + r_o^{2}\, r^{-2})$$

axial component

$$\sigma^{c}_{P_z} = P\, r_i^{2} (r_o^{2} - r_i^{2})^{-1}$$

where σ_{P_e} is a function of the position within the quartz wall, σ_{P_z} is constant as the tensile force producing longitudinal extension of the cylindrical bulb is distributed evenly over the cross-sectional area of the wall.

In the hemisphere there are two equal tangential components.

$$\sigma_{P_\Theta^c} = P\, r_i^3\, 2\,(r_o^3 - r_1^3)^{-1}\,(2 + r_o^3\, r^{-3})$$

The thermal stress components, as a function of radius within the walls, are for a cylinder:

radial component

$$\sigma_{T_r^c} = .5\, W''\, C\, \left[r_i\, \ell n(r/r_i) + r_o^2\, r_i\,(r_o^2 - r_i^2)^{-1} (r_i^2\, r^{-2} - 1)\, \ell n\,(r_o/r_i) \right]$$

$$\sigma_{T_\Theta^c} = .5\, W''\, C\, \left[r_i + r_i\, \ell n\,(r/r_i) - r_o^2\, r_i\,(r_o^2 - r_i^2)^{-1} (r_i^2\, r^{-2} + 1)\, \ell n\,(r_o/r_i) \right]$$

and for the hemispherical section

$$\sigma_{T_\Theta^s} = W''\, C\, \left[r_i - .5\, r_i^2\, r^{-1} - (r_o - r_i)\, r_i^4\, r_o^2\,(r_o^3 - r_i^3)^{-1} (.5\, r^{-3} + r_i^{-3}) \right]$$

$$\sigma_{T_r^3} = W''\, C\, \left[r_i - r_i^2\, r^{-1} + (r_o - r_i)\, r_i^4\, r_o^2\,(r_o^3 - r_i^3)^{-1} (r^{-3} - r_i^{-3}) \right]$$

where C is defined as $\alpha \cdot E \left[(\lambda)(1 - \mu) \right]^{-1}$

The variations in the material constants with temperature were not included in the numerical calculations since the complications introduced would not justify the small increase in accuracy due to the lack of reliable information. For a hemisphere of 54 mm radius we obtain

tangential component at outer wall

wall thickness	2 mm	3 mm
$\sigma^s_{T_{\theta O}}$	4.4 W''	8.0 W''
$\sigma^s_{P_{\theta O}}$	12.0 P	7.9 P

tangential component at inner wall

wall thickness	2 mm	3 mm
$\sigma^s_{T_{\theta i}}$	-6.0 W''	-9.0 W''
$\sigma^s_{P_{\theta i}}$	12.4 P	8.2 P

For the cylindrical part of the envelope which has a 54 mm radius we obtain

tangential component at outer wall

wall thickness	2 mm	3 mm
$\sigma^c_{T_{\theta O}}$	6.2 W''	8.2 W''
$\sigma^c_{P_{\theta O}}$	25.0 P	16 P

tangential component at inner wall

wall thickness	2 mm	3 mm
$\sigma^c T_{\Theta i}$	-6.4 W''	-8.8 W''
$\sigma^c P_{\Theta i}$	26.0 P	17.0 P

axial component at the outer wall

wall thickness	2 mm	3 mm
$\sigma^c P_{zO}$	12.0 P	8.0 P

We can compare the operating stress values to the ultimate strength by evaluating the safety factor (n) which is the ratio of these two numbers.

	Safety Factor, n					
	2mm wall			3mm wall		
stress component	100 psi	200 psi	300 psi	100 psi	200 psi	300 psi
$\sigma^s P_{\Theta O} + \sigma^s T_{\Theta O}$	10.2	5.5	3.8	12.6	7.4	5.2
$\sigma^s P_{\Theta i} + \sigma^s T_{\Theta i}$	14.0	6.2	4.1	30.5	10.9	6.7
$\sigma^c P_{\Theta O} + \sigma^c T_{\Theta O}$	5.3	2.7	1.8	7.8	5.0	3.7
$\sigma^c P_{\Theta i} + \sigma^c T_{\Theta i}$	5.7	4.0	3.1	9.4	5.6	4.0
$\sigma^c P_z$	11.7	5.8	3.9	17.5	8.7	5.8

All of the "n" values are computed with a simulated 50 kW loading, or a W''' value of :

$$W''' \text{ (hemisphere)} \simeq 400 \text{ watts/sq. in.}$$

$$W''' \text{ (cylinder)} \simeq 240 \text{ watts/sq. in.}$$

From these calculations we concluded that an envelope wall of greater than 3 mm has a very excellent chance of meeting our requirements.

5.2 Quartz Enclosure Performance

The initial tests were run on a 3 mm wall dome, straight sided and epoxy sealed to the water-cooled back plate of the FTA source. Cold pressure tests indicated no apparent problems would be encountered due to fatigue effects and operating tests were begun. Of the first two domes tried, one exploded during static pressure tests and the other failed after one minute operation at 18 kW (Figure 25). Both of these enclosures showed surface scratches, bubbles and stress concentrations at the cut-off point. Subsequently, annealed domes with a 4.5 mm wall were purchased to prevent such failures. The next unit tested ran at 20 kW and 40 psi ambient pressure before the epoxy seal overloaded and failed. Post mortem investigation showed a degradation of the seal through thermal overloading by conduction down the quartz. After discussions between Vitro and NASA Houston, the epoxy seal approach was abandoned and a new seal design pursued using a flared end on the dome with a water-cooled, hold-down flange. The arc manifold plate was redesigned to accommodate a flat silicone rubber seal, and to cool this seal with an internal water channel. The flare was set at 21° at the rim with a 4.5 mm wall. Cold static pressure checks indicated that the dome would hold to 200 psi, however, the following two units failed under 100 psi pressure prior to operation of the source. Figure 26 shows the manner in which these domes failed. This failure mode was attributed to out-of-roundness of the dome rim and poor distribution of stresses by the fibre aluminum oxide pad between the clamp ring and the quartz. The next domes were machine-ground to $\pm$ .005 inch tolerance and then fine polished to remove the stresses. The aluminum oxide pad was replaced by a soft copper pad. Preliminary tests were favorable and the system was then completely assembled and prepared for a low power test (35 kW) to check the temperature distribution in the quartz. During this test the shroud sprung a pinhole water lead extinguishing the arc. The dome was unaffected by this failure, permitting the system to be reworked and charged for another test over a 24 hour period. During the ensuing test at 40 kW the silicone gasket overheated, coating the quartz with a black residue. The run was terminated when the quartz temperature reached a measured 900 °C

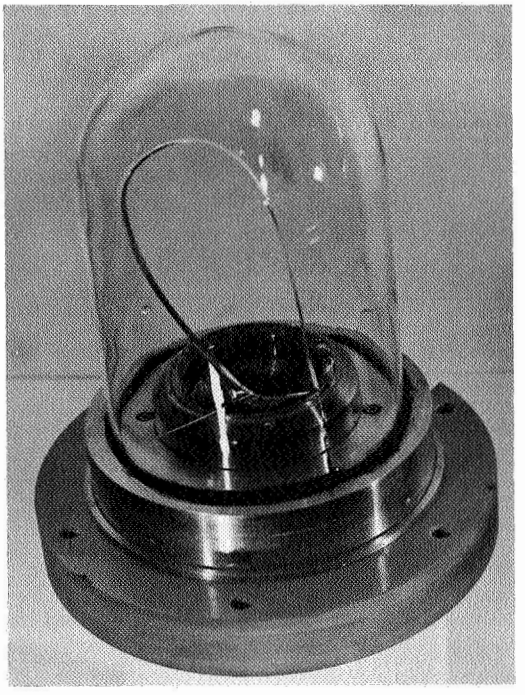

FIGURE 25

QUARTZ FAILURE AFTER ONE MINUTE AT 18 kW

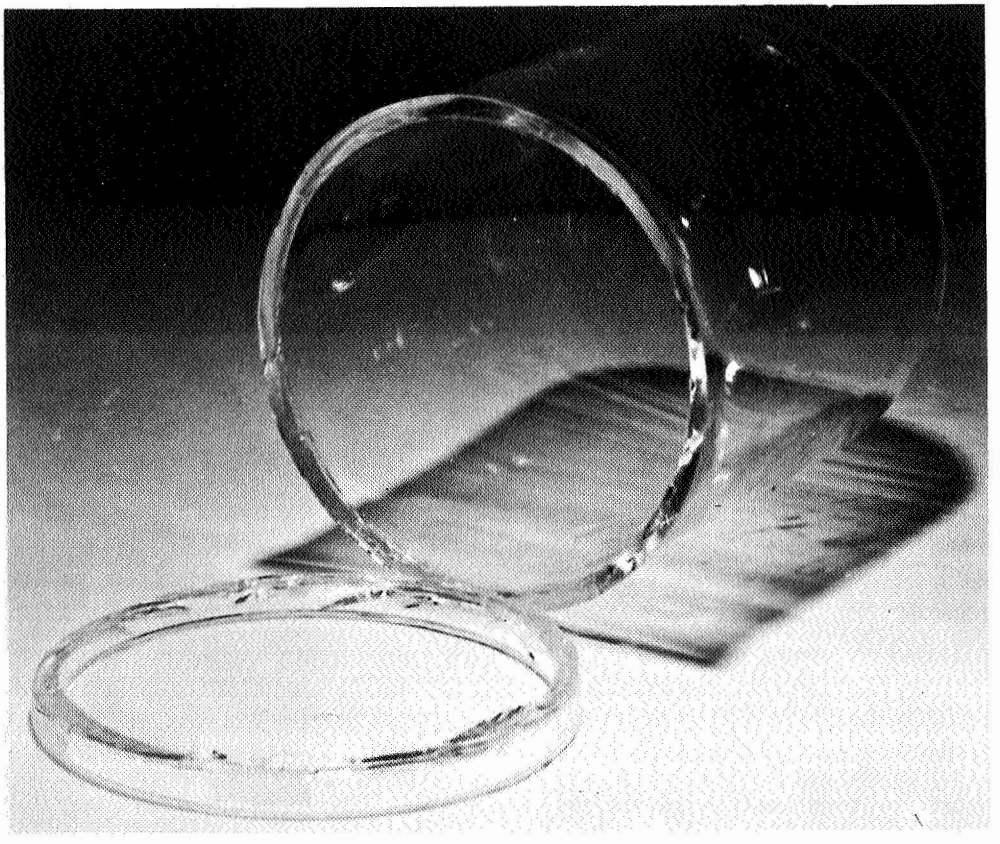

FIGURE 26

QUARTZ FAILURE DUE TO MECHANICAL
STRESS POINTS

at the outside wall. Figure 27 shows the blackened dome with the copper pad still attached to the rim, and Figure 28 shows an end view of the same envelope with the charred silicone gasket.

The following test was made using a silicone rubber gasket with a pure aluminum shield to deflect the hot gases from the area. The test indicated that the quartz temperature was continuously rising, and the run was terminated when the outer wall temperature reached 450°F. These measurements indicated the need for a high temperature seal, or a redesign of the seal area itself to effect cooler operation. Due to the limited time remaining, both of these approaches were pursued simultaneously and both effected a solution.

Several high temperature seal gaskets were fabricated and a set of Parker Inconel-X V-seals were purchased. A soft copper gasket was used first, but did not provide a leak tight joint. The seal was then attempted with a serrated copper gasket filled with soft lead. This seal also failed to provide leak tight operation. On the recommendation of an Allied Chemical Company representative an experimental Teflon seal was used. The material was bronze loaded and had an operating temperature of 750 °F. A dovetail groove was incorpporated in a new head to prevent cold flowing of the Teflon. Again a leak tight seal could not be made due to the need to re-torque the clamping bolts during the first hot run. This was impractical being too near the pressurized high-powered source.

At this time two Parker metal V-seals were received which were rated to 1300 °F and been tested to 200 psig helium at 500 °F with no leakage. The V-ring was fabricated to Inconel-X and silver plated to provide a ductile mating surface. For this assembly the quartz dome was hand lapped to an approximate finish of 4 micro-inches. The brass groove was turned to a machine finish of approximately 10 micro-inches.

The clamping bolts were lapped in and graphite lubricated so that the calculated torques necessary to provide a seal would be reasonably close to the real torques. The unit was assembled and successfully run for 40 minutes. The quartz dome became overheated and softened, due to the lack of circulating air as we steadily increased the input power. The measured equilibrium temperature of the quartz at the seal was approximately 650 °F and the seal was successful.

An 8 hour run using the Inconel-X V-seal was accomplished in a completely closed system. Our measurements indicated that the seal temperature remained between 700 °F and 800 °F on the outside wall during the entire test.

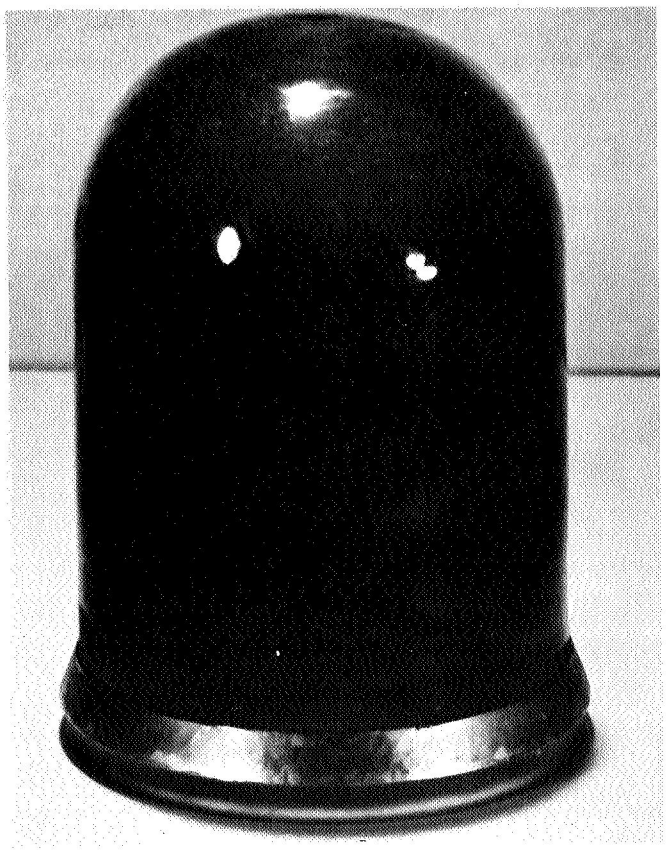

FIGURE 27

QUARTZ DOME AFTER SILICONE GASKET FAILURE

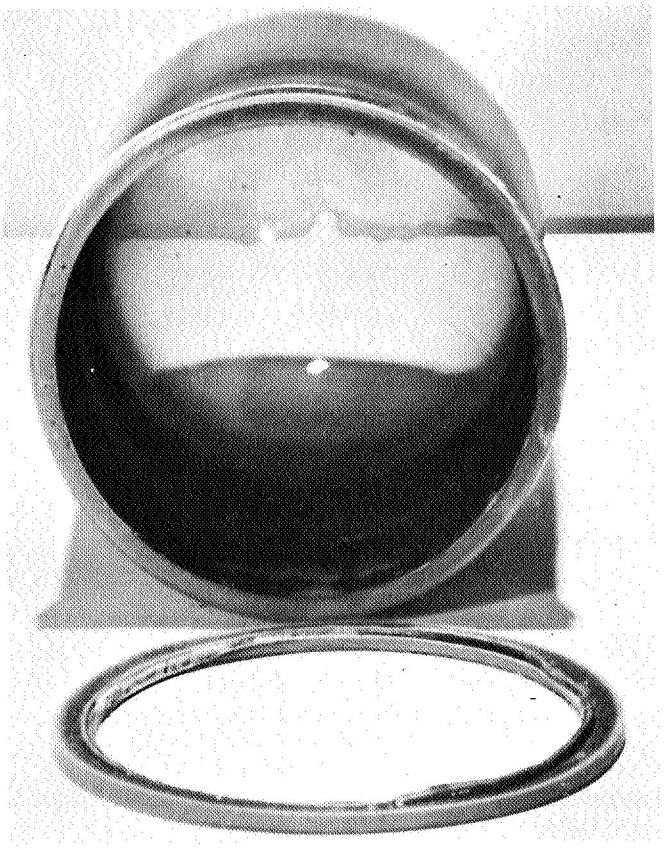

FIGURE 28

END VIEW SHOWING THE DEGRADED SEAL
AND QUARTZ DOME

The seal design used during the successful testing of the complete system in shown in Figure 29. During the test period it became evident that the quartz and the anode shroud regions were becoming contaminated more rapidly than is normal. It was decided therefore not to exceed 35 kW during the test period. A post-test examination showed the tungsten cathode to be cracked and leaking water into the gas system. The results of the test can be summarized as follows: The dome, recirculation system, and seal performed satisfactorily for an 8 hour test period under the severe loading caused by a minute cathode water leak.

Preparations were made after these test results were analyzed to run a 200 hour test. A modified head was prepared with the seal area approximately 1.25 inches further back from the arc than in the previous model. The supplier of the V-ring seal was not able to deliver due to production breakdowns, and the seal was remodified to accept the sister design, an Inconel K-ring, from an alternate supplier. The completed arc-head system with the larger dome and recessed seal position is shown in Figures 30 and 31.

5.3 Fused Seal Studies

A survey of the techniques for making quartz to metal seals was made in order to investigate the possibilities of a graded fuzed quartz, moly flange arrangement. The indications are that this type of seal on a quartz dome is entirely possible, however would be extremely expensive, and in all probability be somewhat of a work of art. This avenue of investigation was then terminated for reasons of impracticality.

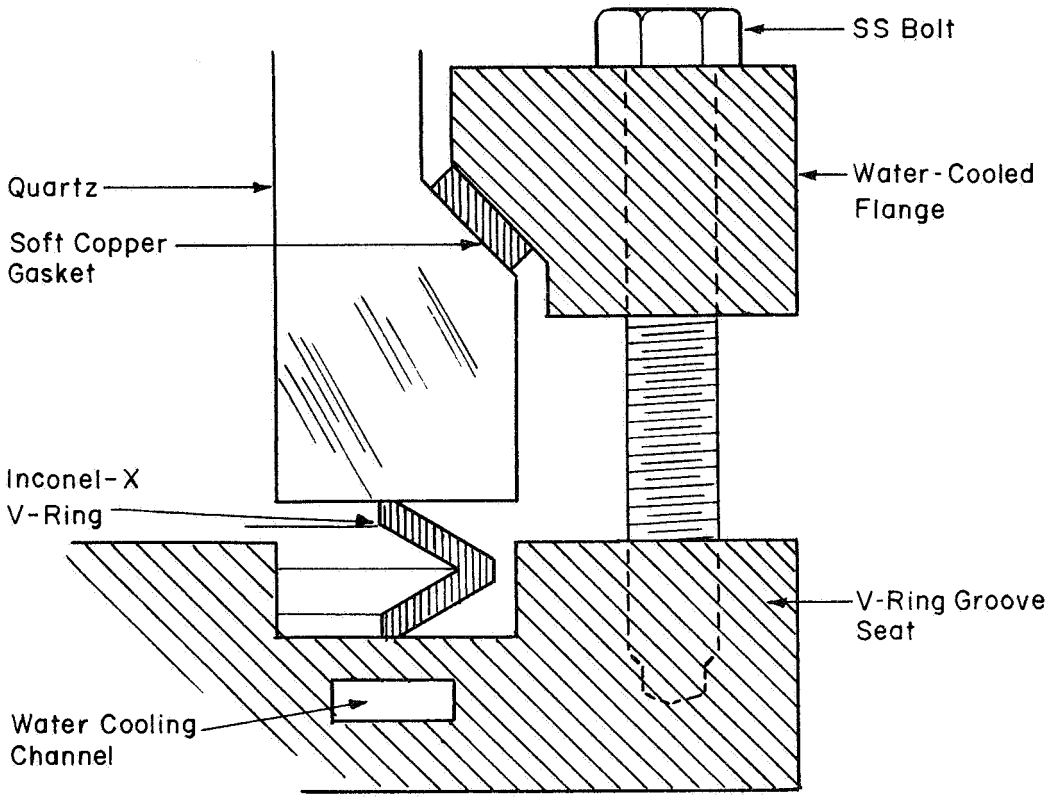

FIGURE 29

INCONEL-X V-RING SEAL DESIGN

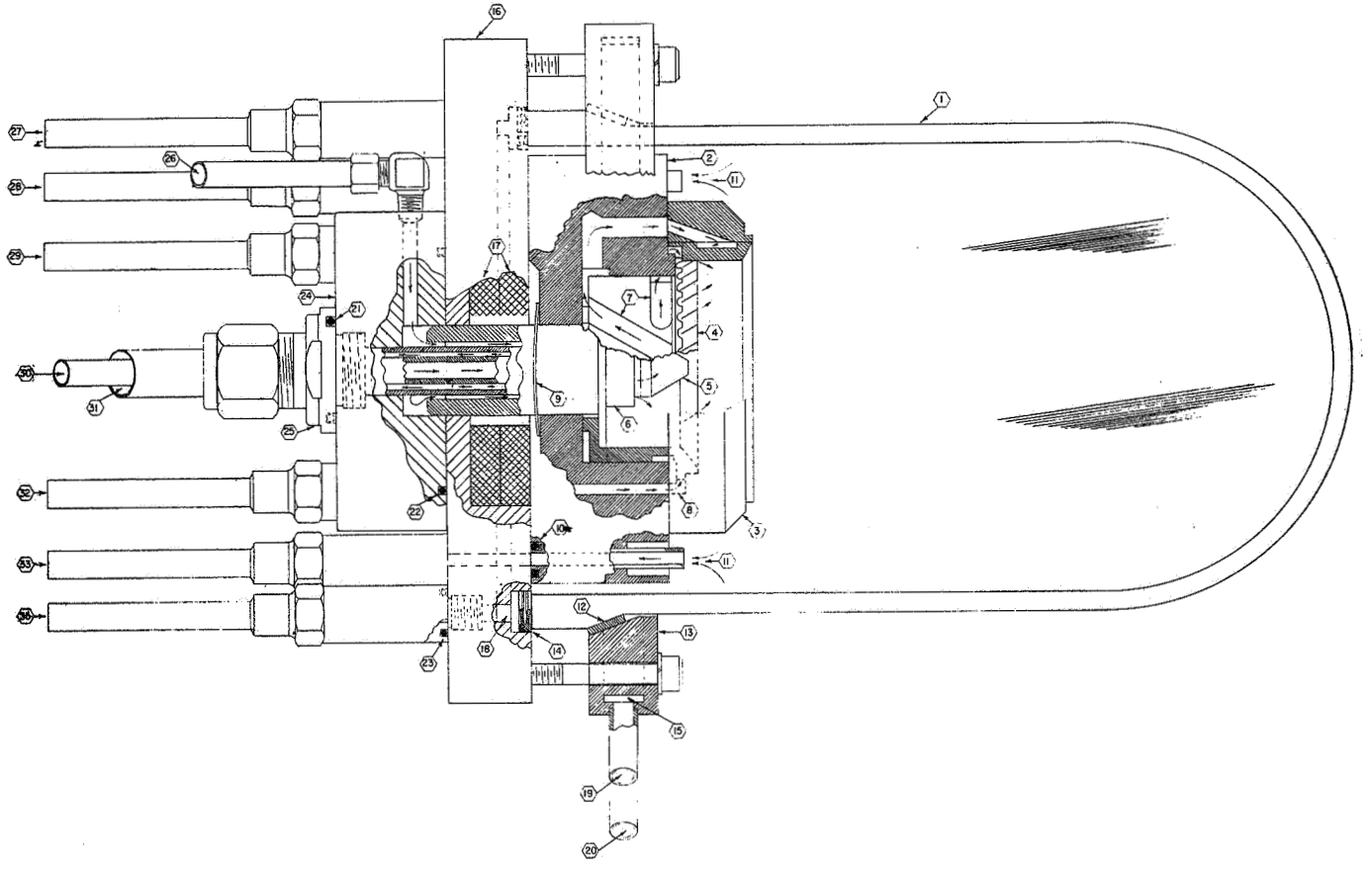

1. Quartz Dome
2. Arc Head Front Section
3. Nozzle Shroud
4. Nozzle (anode)
5. Cathode
6. Cathode Insulator
7. Nozzle and Shroud Coolant Channels
8. Anode Gas Channel
9. Cathode Insulator Retainer
10. Front Head Seals
11. Gas Outlet Ports
12. Copper Gasket
13. Quartz Retaining Clamp Ring
14. Quartz Dome Seal
15. Clamp Ring Coolant Channel
16. Arc Head Rear Section
17. Magnets
18. Quartz Dome Seal Coolant Channel
19. Clamp Ring Coolant Inlet
20. Clamp Ring Coolant Outlet
21. Cathode Holder Seal
22. Cathode Holder Insulator Seal
23. Coolant Connector Seals
24. Cathode Holder Insulator
25. Cathode Holder
26. Cathode Gas Inlet
27. Nozzle and Shroud Coolant Inlet
28. Nozzle and Shroud Coolant Outlet
29. Anode and Cathode Gas Outlet
30. Cathode Coolant Inlet
31. Cathode Coolant Outlet
32. Anode Gas Inlet
33. Dome Seal Coolant Outlet
35. Dome Seal Coolant Outlet

FIGURE 30

REDESIGNED 50 kW ARC HEAD AND SEAL CONFIGURATION

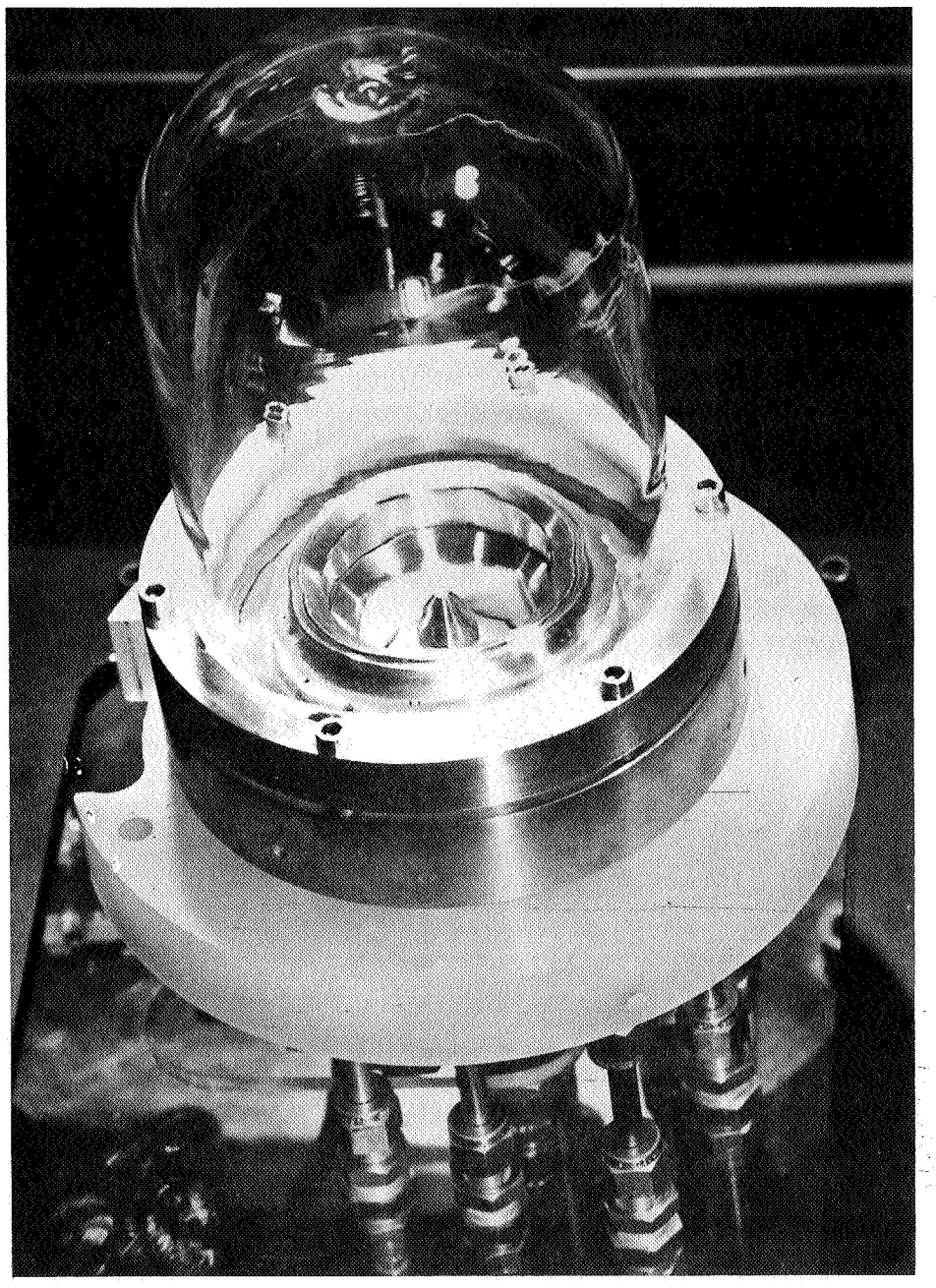

FIGURE 31

ASSEMBLED UNIT PRIOR TO TEST RUN

6. SUMMARY AND CONCLUSIONS

Endurance tests of the arc head alone indicated that this link would perform satisfactorily without interruption and completely without maintenance for 107 hours at power levels over 40 kW. A closed system test was shut down after 45 hours of operation above 40 kW with no imminent failure visible. Short tests indicated that the newly designed quartz dome and Inconel-X V-seal had been debugged and would perform satisfactorily.

Over a two-month period, seven (7) test attempts were made to achieve a longevity run with the system completely integrated. Several of these were false starts due to improper assembly; however, four of these tests were legitimate runs, all of which failed within 8 hours. In the last of these tests, the arc had an 8 hour preliminary run in a chamber with no degradation to check out the head and recirculatory system before the dome was fastened; however, when the dome was fastened this test resulted in the same type of failure as the others. The mode of destruction was a rapid degradation of the anode resulting in copper deposits on the quartz, and finally a puncture of the anode copper itself, shutting down the arc. In no case did a mechanical failure of the quartz enclosure cause termination, nor did seal degradation appear as a problem. We had apparently resolved the design difficulties only to find that in a small enclosure the gas flow pattern is sufficiently changed so as to adversely affect the anode life. The quartz dome enclosure still presents a serious problem in a high-powered arc system.

A system that has proved it will work, however, is the one in which the arc is enclosed in a metal chamber of reasonable volume. In order to use this concept to fulfill solar simulation needs, the configuration shown in Figure 32 is proposed. This system contains the collection optics within the chamber which is part of the closed recirculation system. Because this design concept has been proven feasible in our tests, we recommend strongly that a unit of this type be procured for evaluation at NASA-MSC, Houston.

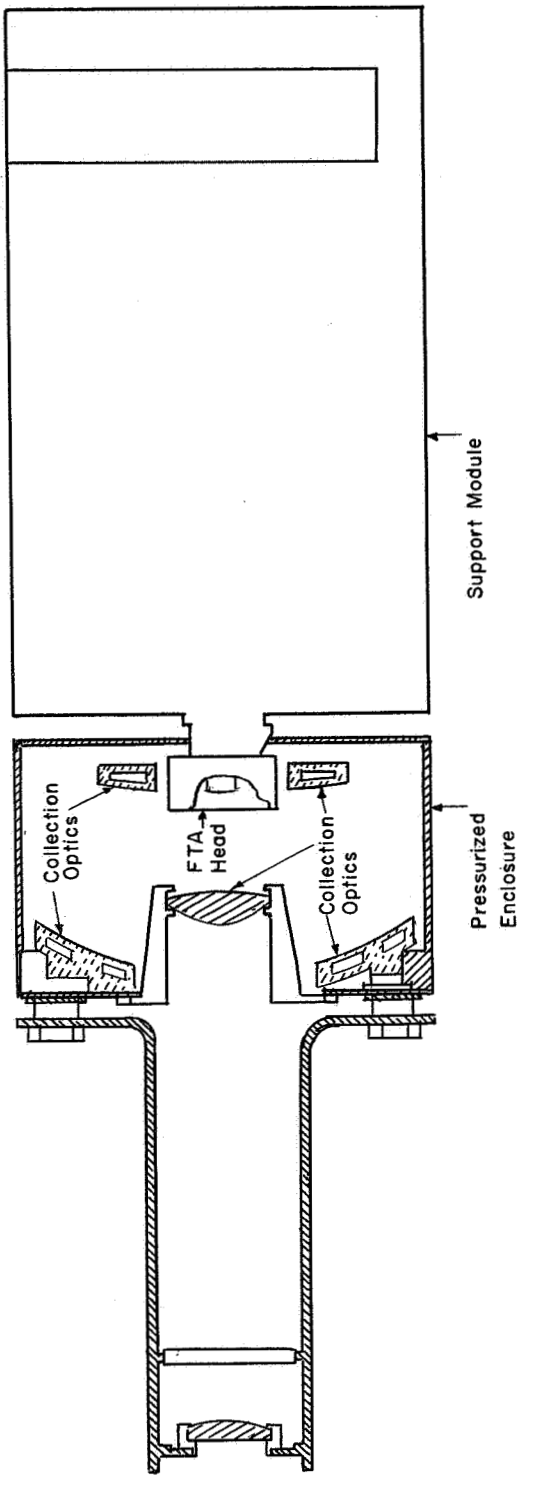

FIGURE 32
PROPOSED SYSTEM FOR NASA-MSC SOLAR SIMULATOR

7. REFERENCES

1. C. Sheer, J. A. Cooney, and D. L. Rothacker
AIAA Vol. 2 No. 3, 483, March 1964

2. AEDC - Technical Documentary Report No. AEDC-TDR-64-251.